

Mediterranean Tropical-Like Cyclones forecasts and analysis using the ECMWF Ensemble Forecasting System (IFS) with physical parameterizations perturbations

Miriam Saraceni¹, Lorenzo Silvestri², Peter Bechtold³, and Paolina Bongiannini Cerlini⁴

^{1,2}Department of Civil and Environmental Engineering, University of Perugia, Perugia, Italy

⁴Department of Physics and Geology, University of Perugia, Perugia, Italy

³European Centre for Medium-Range Weather Forecasts, Bonn, Germany

Correspondence: Miriam Saraceni (miriam.saraceni@unipg.it)

Abstract. Mediterranean Tropical-Like Cyclones, called “medicanes”, present a multiscale nature and their track and intensity have been recognized as highly sensitive to large-scale atmospheric forcing and ~~to~~ diabatic heating as represented by the physical parameterizations in numerical weather prediction. Here, we analyse the structure and investigate the predictability of medicanes with the aid of the European Centre for Medium-Range Weather Forecast (ECMWF) Integrated Forecast System (IFS) ensemble forecasting system with 25 perturbed members at 9 km horizontal resolution (compared to the 16 km operational resolution). The IFS ensemble system includes the representation of initial uncertainties from the ensemble data assimilation (EDA) and a recently developed uncertainty representation of the model physics with perturbed parameters (Stochastically Perturbed Parameterizations, SPP). The focus is on three medicanes, Ianos, Zorbas and Trixie ~~that have been~~ among the strongest in recent years. In particular, we have carried out separate ensemble simulations with initial perturbations, full physics SPP, ~~and~~ with a reduced set of SPP, where only convection is perturbed to highlight the convective nature of medicanes and an operational ensemble combining the SPP and the initial perturbations. It is found that compared to the operational analysis and satellite rainfall data, the forecasts reproduce the tropical-like features of these cyclones. Furthermore, the SPP simulations compare to the initial condition perturbation ensemble, in terms of tracking, intensity, precipitation and more generally in terms of ensemble skill and spread. Moreover, the study confirms that similar processes are at play in the development of the investigated three medicanes, in that the predictability of these cyclones is linked not only to the prediction of the precursor events (namely the deep cut-off low) but also to the interaction of the upper-level ~~dynamically driven~~ advected Potential Vorticity (PV) streamer with the tropospheric PV anomaly that is ~~driven by surface heating and stratiform and convective condensational heating~~ diabatically produced by latent heat.

1 Introduction

The Mediterranean region is a small but geographically complex area characterized by sharp land and sea transitions and surrounded by high mountain ranges. It is known for its frequent cyclogenesis. A small number of the intense cyclones that originate in the region present tropical-like features (Flaounas et al., 2022). They are a very significant phenomenon, due to

their visual similarity with tropical cyclones, and while they are typically shorter-lived than North Atlantic hurricanes, they may exhibit several tropical-like characteristics in their mature phase, such as a high degree of axial symmetry, a warm core, a
25 tendency to weaken after making landfall, and a cloud-free "eye" at the center of the storm of mostly calm weather, as inferred from satellite images. Such vortices are better known as Tropical-Like Cyclones or Mediterranean hurricanes (medicanes). Medicanes have been documented in the Mediterranean region since the beginning of the satellite era (Ernst and Matson, 1983) and have been associated with polar lows (Rasmussen and Zick, 1987). These storms pose a significant threat due to their intense winds, heavy rainfall, and associated flooding.

30

Medicane features have been commonly observed-reported in the literature (Cavicchia et al., 2014; Romero and Emanuel, 2013; Emanuel, 2005; Zhang et al., 2019; Miglietta and Rotunno, 2019). They occur very infrequently, with an average of about 1/2 events per year over the entire Mediterranean region. They are most commonly formed in the western Mediterranean and ~~in~~ the area between the Ionian Sea and the North African coast. Medicanes have a distinct seasonal pattern, with a peak at
35 the start of winter, a significant number of events during fall, a few during spring, and very little activity in summer. As pointed out by Miglietta and Rotunno (2019) they only have a lifespan of a few days due to the limited size of the Mediterranean Sea, which is their main source of energy. Furthermore, they only exhibit fully tropical characteristics for a short period, with extratropical features predominating for most of their lifetime (Miglietta and Rotunno, 2019).

40 Medicanes differ from other Mediterranean cyclones in the complexity of their formation and ~~maintenance. Indeed~~ evolution. However, unlike hurricanes, which develop in regions with near-zero baroclinicity and draw their energy from warm tropical oceans, medicanes form from pressure lows under moderate to strong baroclinicity, which is a typical condition of midlatitudes ~~. The latter aspect leads to a low rate of occurrence, given that the environmental conditions of weak vertical wind shear, which are necessary for their development, are unusual (?). The interaction between warm sea and cold air and~~
45 Mediterranean cyclogenesis. Indeed, medicanes are regarded as baroclinic cyclones evolving into vortices with structural characteristics similar to tropical cyclones (Flaounas et al., 2022). The debate is still open on which processes sustain the cyclone development, baroclinic instability or pure diabatic forcing which also marks the tropical transition phase (Flaounas et al., 2022; Mi

50 Typically, the initial phase of a medicane life cycle is similar to that of an extratropical cyclone, where the medicane intensifies through the interaction of an upper tropospheric disturbance (Potential Vorticity streamer (Flaounas et al., 2015)) with a low-level baroclinic area. However, their development is what makes them different given the relative contribution of large-scale forcing, air-sea interactions, and convection at different stages of their lifetime. Recently a classification has been produced for this type of phenomenon by Miglietta and Rotunno (2019) and Dafis et al. (2020). Medicanes have been grouped
55 into three categories: those where baroclinic instability plays an essential role throughout the cyclones' lifetime and most of their intensification can be attributed to convection; those where baroclinicity is relevant only in the initial stage, and, the theory of wind-induced surface heat exchange (WISHE (Emanuel, 1986)) can explain their intensification through positive feedback

between latent heat release and air-sea interactions, although WISHE may only take place after the occurrence of tropical transition, i.e. after organized convection near the cyclone centre is capable of sustaining the vortex; and finally those, including smaller-scale vortices, that develop within the circulation associated with a deep upper-level trough creates the necessary thermodynamic disequilibrium for these storms to develop a warm core (Emanuel, 2005; Miglietta and Rotunno, 2019). The type of mechanics that can be deemed responsible for the creation of a medicanes in synoptic-scale cyclone.

For this study three medicanes, among the strongest in recent years, were chosen: Ianos (September 15-20, 2020), Zorbas (September 27-31, 2018), and Trixie (October 28-November 1, 2016). The three medicanes have been selected because they are very different from each other, with Trixie being the weakest but also the longest lasting of the Mediterranean is similar to the one responsible for three (Di Muzio et al., 2019; Dafis et al., 2020) and generally among the longest lasting medicanes, Zorbas one of the shortest-lived and presenting high variability in predictability, as documented by Portmann et al. (2020) and Ianos one of the most intense medicanes ever observed, reaching category 2 hurricane status (Lagouvardos et al., 2022). As reported in the literature the three cyclones' origin is linked to the presence of upper-level cutoff low (Comellas Prat et al., 2021) associated with a potential vorticity streamer (Portmann et al., 2020). There, is suggested that the formation of tropical cyclones farther from the equator near the tropics (?).

The development and maintenance of medicanes are the results of a synergy between synoptic-scale processes, which provide the necessary environment, and mesoscale processes such as the cyclone was accompanied by an anomalous value of SST of nearly 1.5 °C (at least in the cases of Ianos (Comellas Prat et al., 2021) and Zorbas (Portmann et al., 2020)). Moreover, the three cyclones acquired tropical-like characteristics in their lifetime: Ianos between the 17th and the 18th of September 2020 (Panegrossi et al., 2023), Zorbas on the 28th of September 2018 (Dafis et al., 2020) and Trixie during the 30th (Dafis et al., 2020). Nonetheless, besides these similarities, the convective activity and processes of intensification that pertain to each cyclone have been recognized to be different in the literature. Dafis et al. (2020) pointed out that Zorbas and Trixie showed long-lasting and organized convective activity close to the centre preceding the maximum cyclone intensity, while Ianos showed deep convection and latent heat fluxes from the sea (Emanuel, 2005), precipitating clouds close to the center during the maximum cyclone intensity (Lagouvardos et al., 2022). Furthermore, there might have been a different contribution in the intensification of the cyclones by baroclinic and diabatic processes, with Ianos influenced mostly by diabatic processes in its intense phase (Comellas Prat et al., 2021) and Zorbas and Trixie developing in a baroclinic environment where convection possibly having a secondary role (Dafis et al., 2020).

Because of their small size, limited data availability, low frequency of occurrence (Cavicchia et al., 2014), and the complex geography of the Mediterranean region, studying and predicting medicanes is a challenge for numerical weather forecasting. For this reason, besides There are some climatological studies on medicanes, using synthetic production of tracks and 3D numerical simulation (Romero and Emanuel, 2013; Cavicchia et al., 2014) there is a higher rate of studies in the literature that has been focused on modeling (Romero and Emanuel, 2013; Cavicchia et al., 2014; Zhang et al., 2019) which have assessed the climatological medicanes number per year, seasonal pattern, areas of occurrence and intensity. There are fewer studies based on observations (Pytharoulis et al., 2000; Moscatello et al., 2008; Miglietta et al., 2013) given the above-mentioned low

frequency of occurrence and scarcity of data, which were focused on the analysis of medicanes convective activity. Numerous modeling studies of medicanes using convective permitting models, ~~due to the fact that they can be more effective at reproducing~~ the and general circulation models include Davolio et al. (2009); Miglietta et al. (2011, 2013); Mazza et al. (2017); Cioni et al. (2016); Ricci et al. (2016); Ricci et al. (2017); Ricci et al. (2018); Ricci et al. (2019); Ricci et al. (2020); Ricci et al. (2021); Ricci et al. (2022). Among the others, Carrió et al. (2020) was able to capture, with high-resolution modeling (2.5 km) the development of a small-scale processes that contribute to medicane formation and maintenance (Davolio et al., 2009; Miglietta et al., 2011, 2013; Mazza et al., 2017; Cioni et al., 2016; Ricci et al., 2016; Ricci et al., 2017; Ricci et al., 2018; Ricci et al., 2019; Ricci et al., 2020; Ricci et al., 2021; Ricci et al., 2022), cyclone and its relationship to convection, especially highlighting the role of diabatic heating in its intensification. Cioni et al. (2018) found out that explicit convection is necessary to capture the track, intensity, and thermal structure of a specific medicane in 2014. However, in the above-mentioned review paper, it is concluded that: "...a systematic gain from kilometer-scale resolution has not been generally demonstrated for cyclones yet".

95 ~~There~~ Lastly, there have been relatively few studies that have analyzed medicanes using ensemble forecasts (Chaboureau et al., 2012; Mazza et al., 2017) and more specifically, by using the ECMWF ensemble forecasting system (Pantillon et al., 2013; Di Muzio et al., 2019; Portmann et al., 2020). ~~Indeed~~ Nonetheless, the ensemble forecast of ECMWF has proven to be a useful tool for predicting extreme weather events (Buizza and Hollingsworth, 2002; Buizza, 2008; Magnusson et al., 2015), for analyzing tropical cyclones (Torn and Cook, 2013) and their predictability (Munsell et al., 2013). Moreover, the model has demonstrated high predictive skill also for medicanes (Di Muzio et al., 2019). Pantillon et al. (2013) used ECMWF operational ensemble forecasts to study the predictability of a medicane in 2006 and found that they were more successful at consistently capturing early signals of its occurrence compared to ECMWF deterministic forecasts. However, Di Muzio et al. (2019), who used ECMWF ensemble forecasts to systematically analyze the predictability of medicanes, found that the ensemble members noted a marked drop in predictive skill beyond 5-7 lead days, indicating the existence of predictability barriers. Portmann et al. (2020) used ensemble forecasting to assess upstream uncertainties in the prediction of medicanes, ~~finding also~~ finding that the uncertainties were reduced with ~~later initializations~~ initialization closer to the medicane occurrence.

Research conducted on medicanes with ensemble forecasting has generally been carried out through the use of the perturbations to initial conditions only (~~Di Muzio et al., 2019; Portmann et al., 2020~~), as in Di Muzio et al. (2019), without the use of parameterization perturbations, by means of any stochastically perturbed parameterization scheme. However, an important part of the uncertainty associated with forecasting comes from uncertainty related to the physics of the model. For these reasons, this present study is concerned with ensemble forecasting that takes into account not only the uncertainty of initial conditions but also the uncertainty of model parameters. We present an assessment of the prediction of medicanes, with the use, not only of the ~~Integrated Forecasting System (IFS)~~ IFS operational ensemble forecasting system at ECMWF, with initial conditions perturbation, but using also the physical parameterization perturbations, the Stochastically Perturbed Parameterizations (SPP) ensemble forecast. Indeed, this is a novel ~~scheme of~~ stochastic representation of model uncertainties which is still under development at ECMWF in order to replace the Stochastically Perturbed Parameterization Tendency scheme (SPPT) (Palmer et al., 2009).

SPP has been found relevant in improving forecasts, specifically with ECMWF ensembles (?) and tropical cyclones. This new representation of uncertainties associated with model physics consists of a set of physical parameters in the model being perturbed (Ollinaho et al., 2017). The use of this method is rising in the literature (Frogner et al., 2022) precisely because added value of SPP is that it perturbs the amplitude and the shape of the tendencies from the individual physical processes, thereby also allowing for the generation of clouds and convection, thus it does not only perturb the amplitude of the total physics tendency as with SPPT. Leutbecher et al. (2017) and Lang et al. (2021) report on skillful forecast with SPP in the ECMWF ensemble system including for tropical cyclones, where SPP increases the spread of the tropical cyclone core pressure while presenting similar statistics to SPPT for the cyclone tracks. As discussed in Frogner et al. (2022) ensemble applications using SPP are clearly on the rise as it allows the reproduction representation of uncertainty close to the actual source of error and maintains physical consistency, particularly with local conservation of energy and humidity (Lang et al., 2021).

Thus, a comparison between three ensemble forecast experiments is set up. One ensemble is run with only initial condition perturbations, through the Ensemble Data Assimilation (EDA), one is run with the entire physical parameterizations perturbed and one is run with only the convective parameterization perturbed. The last experiment comprises both the initial conditions and the model parameterizations perturbations. Each of these experiments is applied to the three above-mentioned chosen medicanes and the goal of this study is to determine whether these forecasts can accurately predict medicanes and them, if there are possible biases presented by the ensemble forecasts. The goal of the research is also to assess and if the ensembles compare in terms of spread and error. Furthermore, the assessment of which of the perturbation experiments can capture the medicane more accurately and is carried out trying also to understand what physical diabatic processes, among the ones already studied in the literature, influence the forecast and how these are predicted by different ensembles different ensembles predict these.

Differently from Di Muzio et al. (2019), only three medicanes, among the strongest in recent years, were chosen: Ianos (September 15-20, 2020), Zorbas (September 27-31, 2018), and Trixie (October 28-November 1, 2016). The three medicanes have been selected because they are very different from each other, with Trixie being the weakest but also the longest lasting of the three (Di Muzio et al., 2019) and generally among the longest lasting medicanes, Zorbas one of the shortest-lived and presenting high variability in predictability, as documented by Portmann et al. (2020) and Ianos one of the most intense medicanes ever observed, reaching category 2 hurricane status (Lagouvardos et al., 2022).

In section The outline of the paper is the following. In Section 2 the data and methods used are described, with an in-depth description of the ensemble forecast experiments carried out, a description of the SPP, and of the tracking method. In section 3 a brief overview of the three storms studied is provided, highlighting their important characteristics. In section 4 the results are presented for the track position and, and of the Hart (2003) diagnostic. In Section 3 the assessment of the ensemble predictions of medicanes in terms of tracking, intensity, precipitation, and thermal structure. In the final section is presented. Then, in Section 5 the relevant process involved in the evolution and prediction of the medicanes are investigated in relation to the results of the previous sections and in Section 6, the results are discussed and the concluding remarks are given.

2 Data and Methods

165 ~~In this section, a description of the methods and techniques used to analyze the medicanes with the ensemble forecast and the operational analysis with the ECMWF model Integrated Forecasting System (IFS), is given. Firstly, a description of the Stochastically Perturbed Parameterizations ensemble forecast of IFS is provided, together with a brief description of the carried-out perturbation experiments. Secondly, the data, used to validate the simulation besides the operational analysis, are described. Finally, the tracking algorithm is described.~~

2.1 Ensemble Forecast Simulation

170 For this work, the ensemble forecast experiments with the ECMWF IFS (Cycle 47r3: ECMWF, (IFS Documentation CY47R3, 2021b)) and the ECMWF operational analysis have been used. Both the ensemble forecast and the operational analysis have a ≈ 9 km horizontal grid spacing (TCO1279, for a more in-depth description of the horizontal grid, see Malardel et al. (2016)) and ~~are run with 137 vertical levels.~~ The forecasted period levels in the vertical. The duration of the simulations used in this work is 9 days. Three different sets of experiments have been conducted, all of them consisting of ~~an 24-members~~ a 24-member 175 ensemble. The ensemble forecasts are initialized, amounting to 3 initial dates, each day at 0000 UTC. For Ianos the three dates are the 15th, the 16th, and the 17th of September 2020, for Zorbas the three dates are the 25th, the 26th, and the 27th of September 2018 and for Trixie, the three dates are the 25th, the 26th, and the 27th of October 2016. The three dates were chosen as three days before the intensification phase of each cyclone, based on the reference data of ERA5 reanalysis. Regarding the physical parameterization, a detailed description can be found in the IFS documentation (IFS Documentation CY47R3, 180 2021a). ~~The ensemble forecasts are~~ The ensemble forecast is coupled to the ECMWF Wave Model (ecWAM: (IFS Documentation CY47R3, 2021c)) ~~, and~~ to the Nucleus for European Modelling of the Ocean (NEMO) ocean model (Mogensen et al., 2012) ~~and the LIM2 sea ice model (?).~~ ~~The Different.~~ The ecWAM model provides the atmospheric model with the Charnock parameter, thus controlling the sea surface fluxes via the surface roughness. The atmospheric oceanic surface heat and moisture fluxes are controlled by 185 the SSTs computed from NEMO every 20 minutes using a 0.25° horizontal grid with 75 vertical levels. Due to the limited horizontal resolution of NEMO, the IFS is forced in the middle latitudes only, with fixed SSTs from the OSTIA product (Donlon et al., 2012) up to day 4, while beyond day 4 the SSTs from NEMO are used. The different types of experiments that have been carried out are reported in Table 1.

The first experiment is the ensemble forecast with initial condition perturbation only (INI experiment). This is done by adding 190 perturbation to a 4D-Var (Rabier et al., 2000) analysis. The perturbations are constructed from an ensemble of 4D-Var data assimilations (Ensemble Data Assimilation, EDA, (Buizza et al., 2008)) where the size of the initial perturbations stems from the analysis uncertainty due to observation errors and model uncertainties including SPPT in the trajectory of the variational data assimilation. The second and third sets of experiments are conducted by running the ensemble with ~~SSP-SPP~~ applied. In the former (SPP-Conv) only the convective parameterization parameters are perturbed. In the latter (SPP), the ~~whole physics~~ 195 ~~parameterization, convection, radiation, convective, radiative,~~ clouds and large-scale precipitation ~~and turbulence diffusion,~~

Table 1. Description of the different ensemble forecast experiments

Experiment ID	Experiment Setup
<i>INI</i>	Initial perturbations only - no model uncertainty representation
<i>SPP – Conv</i>	No initial perturbations - convective parameterization uncertainty representation
<i>SPP</i>	No initial perturbations - physical parameterizations uncertainty representation
<u><i>TOT</i></u>	<u>Initial perturbations - physical parameterizations uncertainty representation</u>

turbulence, diffusion, and sub-grid orography parameters-parameterization parameters of the IFS model are perturbed, as briefly discussed below. In the last experiment (TOT) the operational forecast conditions of ECMWF are tested by including both the initial condition perturbation and the physical parameterizations perturbation.

2.2 Stochastically Perturbed Parameterizations Ensemble

200 The Stochastically Perturbed Parameterizations scheme represents model uncertainty in numerical weather prediction by introducing stochastic perturbations into the physical parameterization schemes (Lang et al., 2021) as mentioned above. SPP is a new scheme, aimed at replacing the currently used Stochastically Perturbed Parameterization Tendency scheme (SPPT) (Palmer et al., 2009) in the ECMWF ensemble forecast in June 2023. The new scheme, developed by Ollinaho et al. (2017), following the work of ~~Baker et al. (2014); Christensen et al. (2015)~~Baker et al. (2014) and Christensen et al. (2015), is based

205 on applying perturbations directly to ~~well-known poorly constrained parameters and variables~~a selected number of parameters and/or equations within the parameterization schemes. ~~This way the model uncertainty representation can be directly related to known sources of model uncertainties associated with specific processes. Thus, with the SPP, some individual IFS parameters and variables are perturbed at each timestep with in-space varying noise derived from in-time evolving 2D random number fields, usually those known to be specific sources of uncertainty for the model. The perturbations follow horizontal patterns that~~

210 evolve stochastically in space and time. Each perturbed parameter is assigned an individual random field and different random fields are statistically independent. The log-normal distribution has been chosen for practical reasons as it ensures that the perturbed parameter values retain their original sign. The ~~SPP scheme is designed such that it converges to the unperturbed (i.e. deterministic) forecast model in the limit of vanishing variance of the noise.~~ The implementation of SPP allows ~~simultaneous perturbations~~the simultaneous perturbation of up to 27 parameters and variables in the deterministic IFS parametrizations of

215 turbulent diffusion (Köhler et al., 2011), ~~subgrid~~sub-grid orography (Beljaars et al., 2004), convection (Tiedtke, 1989; Bechtold et al., 2008), cloud processes and large-scale precipitation (Tiedtke, 1993; Forbes et al., 2011), and radiation (ecRad, (Hogan and Bozzo, 2018)). These 27 parameters and variables are reported in Supplementary Tables 1 to 4, together with a

~~thorough explanation~~ detailed explanation of the choices behind their perturbation. As mentioned above, the SPP perturbation is applied through a 2D random field generator. In its implementation, SPP uses a single scale with a decorrelation length scale of 1,000 km and a decorrelation time of 3 days (~~Figure~~ Fig. 1 of Lang et al. (2021)).

2.3 Validation Data

In order to analyze the predictive skill of the ensemble, besides the operational analysis, the ensemble forecast perturbation experiments have been compared with the satellite-based, globally-gridded Global Precipitation Measurement (GPM) Integrated Multi-satellite Retrievals for GPM (IMERG) (Huffman et al., 2020). In GPM-IMERG, the retrievals from geostationary satellites are blended seamlessly with information from the passive microwave (PMW) sensors from low-orbit satellites. this is done in order to ~~provide for~~ achieve both a high accuracy and a high temporal (30 min) and spatial ($\simeq 10$ km) resolution since the precipitation estimation based on ~~only the PMW~~ the PMW alone suffers from a low sampling rate. Furthermore, the data are also calibrated by using rain gauges at the ground baselevel. In this research, the ~~24-hr~~ 24-hour accumulated precipitation values are used. The latter data are provided at the same resolution, 0.1° , ~~of as in~~ the ensemble simulation.

2.4 Cyclone tracking

The method described here has been used to evaluate the tracks for both operational analyses, used as verification and ensemble forecasts. The tracking method is based on Picornell et al. (2014) and Ragone et al. (2018). The algorithm ~~is firstly aimed~~ first aims at finding the local minima of the sea level pressure field at each time step. Then, for each minimum, the sea level pressure gradient of the sea level pressure along eight ~~principal-main~~ directions (E, NE, N, NW, W, SW, S, SE) ~~inside~~ within a circle of radius 200 km is computed. The computed gradient is then chosen to be lower than $5hPa/200km$ in at least 6 directions. After the minimum detection and filtering via selection through ~~sea~~ sea level pressure gradient, a proximity condition is applied to construct the complete trajectory. Starting from the first ~~time-step~~ time step, each minimum is connected to the following one, at the following ~~timestep, that respect~~ time step, that satisfies the condition of being closer than $\Delta x = V\Delta t$, with $V = 50km/h$ and $\Delta t = 3h$. If this condition is met, the two consecutive minima are considered to belong to the same trajectory. This condition ~~has been was~~ considered suitable and chosen according to the results of Ragone et al. (2018). Once the trajectories have been found, only the trajectories that last longer than 24 hours and those that spend more than 12 hours over the sea are selected. Trajectories that spend less than half their ~~duration~~ time over land or within 100 kilometers of the coast ~~will be discarded~~ are discarded.

2.5 Hart Parameters

To analyze these three storms, the thermal structure, and the thermal asymmetry have been investigated. The chosen parameter to quantify the latter has been recognized in the upper-level thermal wind, $-V_T^U$, which is considered to be a relevant parameter in distinguishing tropical-like cyclones from fully baroclinic cyclones (Mazza et al., 2017), and secondly on the thermal

250 asymmetry, B . These parameters belong to the three-dimensional cyclone phase space diagnostic introduced by Hart (2003). There, the thermal asymmetry is defined as the storm-motion-relative 900–600 hPa thickness asymmetry across the cyclone within its radius:

$$B = \frac{\overline{(Z_{600 \text{ hPa}} - Z_{900 \text{ hPa}})}_R - \overline{(Z_{600 \text{ hPa}} - Z_{900 \text{ hPa}})}_L}{\overline{(Z_{600 \text{ hPa}} - Z_{900 \text{ hPa}})}_{600 \text{ hPa}}} \quad (1)$$

where Z is the geopotential height, R indicates the right of current storm motion, L indicates the left of storm motion, and the overbar indicates the areal mean over a semicircle around the cyclone centre.

255

Instead, the cyclone's upper-level thermal structure (i.e., its cold or warm core) is indicated by $-V_T^U$. If it attains a positive sign, the cyclone attains an upper-level warm core. Indeed the $-V_T^U$ is defined as:

$$-|V_T^U| = \frac{\partial(\Delta Z)}{\partial \ln(p)} \frac{300 \text{ hPa}}{600 \text{ hPa}} \quad (2)$$

260 The two pressure levels have been changed from 600 hPa to 700 hPa and from 300 hPa to 400 hPa due to the lower height of the tropopause in the midlatitudes with respect to the tropics (Picornell et al., 2014). These values are computed within a 200 km radius around the detected cyclone center by using the geopotential height field. In the Hart (2003) formulation, this radius was chosen to be 500 km, but given the smaller size of medicanes compared to tropical cyclones (Miglietta et al., 2013), the radius used in this study is smaller, 200 km. Since a positive value of lower-level thermal wind, $-V_T^L$, can characterize not only medicanes but also extratropical cyclones with warm seclusion (Hart, 2003), we consider important only the upper-level thermal wind, $-V_T^U$. In the case of the thermal asymmetry, the threshold value of $B = 10 \text{ m}$ has been determined by analyzing ECMWF reanalyses ERA40 at 1.125° of the resolution, from which no major hurricane (winds of greater than 210 km/h) had associated with it a value of B that exceeded 10 m (Hart and Evans, 2001). Even if the threshold value of B has been originally determined for larger tropical/extratropical cyclones, previous studies have shown that such value is also useful in the case of medicanes (Miglietta et al., 2011). The deep warm core phase is represented by the asymmetry B being lower than 10 and closer to 0 and by a highly positive value of $-V_T^U$.

270

3 Overview of the Storms

~~In this section, an overview of the three medicanes chosen is given. A brief analysis of the synoptic environment is provided, following the literature.~~ A summary of the main features as retrieved by the analysis data: the storm duration, the period, the region of occurrence and, the asymmetry B , and upper-level thermal wind $-V_T^U$ (the last two parameters will be explained in the following sections) is provided in Table 2. The latter two parameters have been used for the computation of the cyclone phase space diagrams. The intensity (central pressure) and trajectory of each storm are shown in Figure Fig. 1 along with the ensemble tracks track.

3.1 Ianos

Table 2. Duration, region of occurrence, central pressure, CP, asymmetry parameter, B, and upper-level thermal wind from the operational analysis for each storm. The upper-level thermal wind, $-V_T^U$ and the thermal asymmetry parameter, B are taken from the [Hart eyelones cyclone phase-space of](#) (Hart, 2003).

Storm	Region	Period	Duration (d)	CP (hPa)	B	$-V_T^U$
Ianos	SM	September 2020	7	994	0	73
Zorbas	SM	September/October 2018	5	993	4	39
Trixie	SM	October 2016	4	1009	2	38

*SM = Southern Mediterranean

280 [The three storms formed and developed in the same area, the Southern Mediterranean, in the Ionian and Aegean Seas. This region has one of the highest medicanes occurrences, as recognized in the literature \(Cavicchia et al., 2014; Zhang et al., 2021\). They occurred in the same period of the year, between September and November, the most frequent period for medicane occurrence \(Romero and Emanuel, 2013\). From Fig. 1 it can be gathered that there are some differences in duration and intensity, with Trixie being the longest-lasting of the three medicanes \(in terms of the deepening phase\) and Zorbas and Ianos being deeper than Trixie, as mentioned in the Introduction. As the track suggests \(Figure Fig. 1a\) Ianos originated in the Gulf of Sidra after an upper-level cutoff low that formed on the 9th of September moved eastward to the western Mediterranean and northern Africa. Then between the 14th-15th of September 14th and 15th of September 2020, it emerged in the Gulf of Sidra, due to stratospheric dry intrusion with high vorticity values \(Comellas Prat et al., 2021\). This process was also accompanied by an anomalous value of SST which was 1.5 °C higher than the normal \(27-28 °C\).](#)

290 [On the 16th of September, it intensified, and it moved to the Ionian sea, and then and spent most of its life over the Mediterranean Sea, eventually reaching Greece on the 17th of September, the system showed a clear mid-level warm core, lining up with the cut-off low. Ianos obtained tropical characteristics at this point \(CP = 994, B = 0, and \$-V_T^U = 73\$ \), and turning southeastward, dissipating around the 21st. The analysis is capable to reproduce of reproducing a value similar to the observed pressure minimum of 995 hPa \(Comellas Prat et al., 2021\).](#)

295 3.1 Zorbas

[Zorbas formed at 12:00UTC on 27 Zorbas formed on the 27th of September 2018 close to north-North Africa and then moved into the central Mediterranean, turning eastward and moving over Greece into the Aegean Sea, where it finally decayed 4 d-four days after its formation \(Figure Fig. 1d\). Medicane Zorbas originated from a PV streamer created by the elongation of a large-scale trough in eastern Europe, which reached the central Mediterranean Sea at 00:00UTC on 27 September 2018 \(Portmann et al., 2020\). This PV streamer broke up at the time of cyclogenesis, resulting in the formation of a PV cutoff.](#)

300 [At the same time, as for Ianos, a large SST anomaly was taking place in the Gulf of Sidra, with similar intensity as in the Ianos case. Zorbas cyclogenesis was also accompanied by a strong low-level advection of air with low virtual potential](#)

temperature, Θ_e , across the Aegean sea. Then this air was substantially moistened by sea-surface fluxes as it traveled across the Aegean Sea. One day after formation (28th of September), Zorbas presented a deep warm core (Table 2). After reaching the state of the warm core when Zorbas reached Greece on 29 September 2018, this was sustained for the next few days. Zorbas reached Zorbas reached its maximum intensity (observed 992 hPa), which is well captured by the analysis.

3.1 Trixie

Medicane Trixie formed on the 28th of October, as the consequence of a deep cut-off low which emerged on 26–27 October and moved from northern to southern Italy in the following days, triggering deep convective storms along the Italian west coast. This PV anomaly crossed the Adriatic Sea on 28 October at 04:00 UTC (EUMETSAT analysis by Scott Bachmeier, Joehen Kerkmann, and Djordje Genic) and then quickly moved to Sicily and approached Tunisia and Algeria. Then between the 26 and the 28 of October, the medicane started to develop in the area of the old PV anomaly. 2016. On the 29th of October, it deepened and, it moved to the east of Malta, then on the 30th of October, it moved eastward towards Greece (Figure Fig. 1g) : Trixie reached the warm core structure on the 30th of October. This is in line with observation (EUMETSAT report). Eventually, it passed near Crete on the 31st of October. The most intense convective activity started after 12 h of 30 October 2016 and lasted until 31 October 2016 (Dafis et al., 2020). while dissipating. In the analysis, there was only a short intensification period evident, and the minimum pressure was fluctuating between 1010 and 1014 hPa during the period from the 29th and the 30th of October, which might have been highly underestimated.

The three storms formed and developed in the same area, the Southern Mediterranean, in the Ionian and Aegean Seas. This region has one of the highest medicanes occurrences, as recognized in the literature (Caviechia et al., 2014; Zhang et al., 2021). They occurred in the same period of the year, between September and November, the most frequent period for medicane occurrence (Romero and Emanuel, 2013). From Figure 1 it can be gathered that there are some differences in duration and intensity, with Trixie being the longest-lasting of the three medicanes (in terms of the deepening phase) and Zorbas and Ianos being deeper than Trixie.

4 Results: Ensemble forecast evaluation

This section examines the ensemble forecast experiments for certain aspects that are crucial for cyclones. The primary focus is on focus is put on the cyclones track, the cyclone track, as it is largely influenced by large-scale processes and is therefore a direct reflection of the model's capability to reproduce multi-scale processes. The second feature under investigation is the cyclone's cyclones intensity, as measured by central pressure. This (this value is considered the most stable and robust metric for assessing the intensity of a cyclone on a global scale (Davis, 2018). Then the precipitation is analyzed. To conclude the analysis, the thermal structure and asymmetry have been evaluated by focusing on the asymmetry and the), the cyclones precipitation and thermal structure. The chosen parameters to quantify the latter are the above-mentioned upper-level thermal wind parameters, belonging to the cyclone phase-space theory of Hart (2003). Eventually, the vertical profiles of vorticity,

335 divergence, and heating around the cyclone centre are investigated in comparison with the results of the above-mentioned parameters, $-V_T^U$ and thermal asymmetry, B . Finally, the focus has been put on the process behind cyclone formation and intensification to understand the results of the ensemble simulations. tropical-like phase of these cyclones is thoroughly investigated.

4.1 Tracking

340 The ensemble tracking results are reported in Figure Fig. 1. As examples, the tracks starting from the 16th of September are shown for Ianos, the ones starting from the 27th of September are shown for Zorbas, and the ones starting from the 27th of October are shown for Trixie.

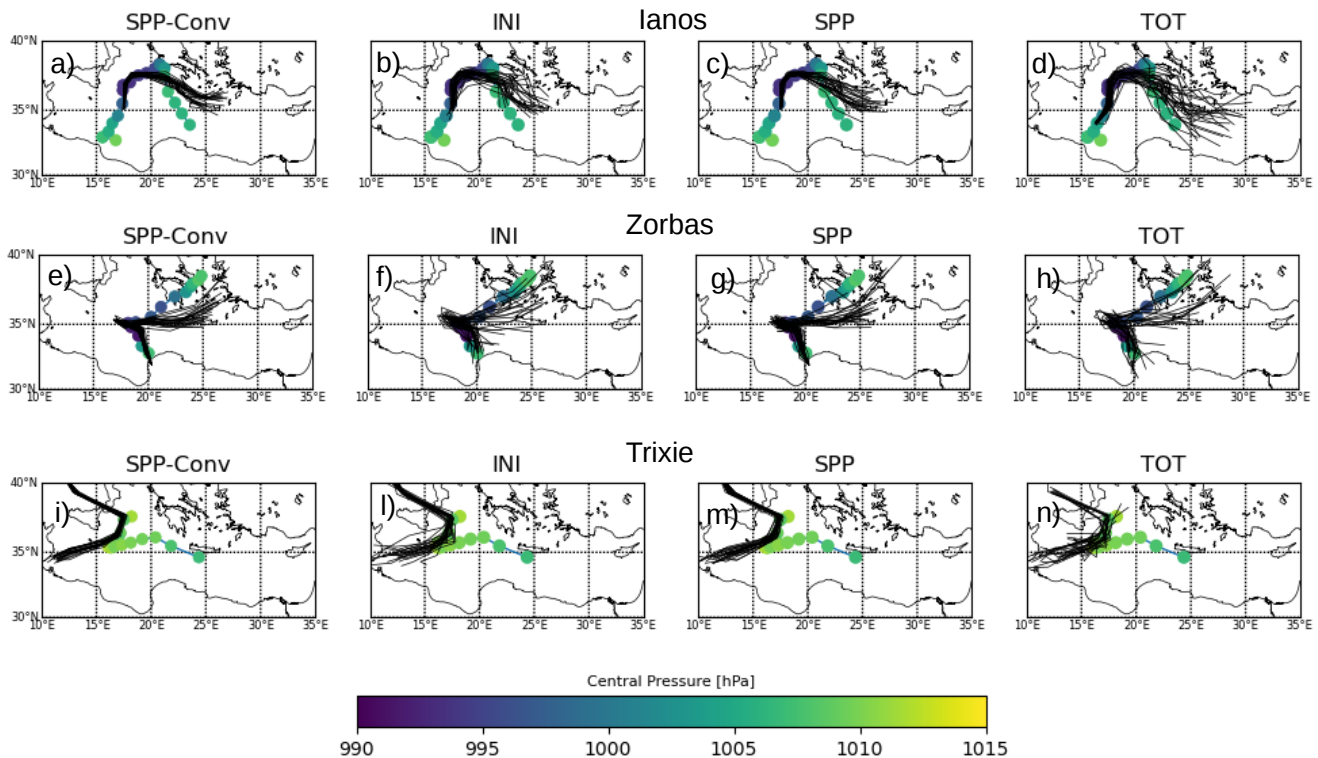


Figure 1. Track of the three storms for the operational analysis as reference track and for the ensemble members belonging to each experiment (SPP-Conv on the first column, INI on the second column and SPP on the third column and TOT in the fourth column) for the three storms, Ianos in a, b and c and d, Zorbas in e, f, g and h and Trixie in i, j, k, l, m and n. As background the operational analysis is reported with the colours representing the intensity, meaning the central pressure in hPa. For Ianos the experiments starting on the 16/09 have been chosen, for Zorbas the ones starting on the 27/09 and for Trixie the ones starting from the 27/10.

By looking at Figure Fig. 1a to e and Figure 1d to f and Fig. 1e to h the ensemble tracks follow sensibly the references for Ianos and for Zorbas. On the contrary for Trixie, the tracking, which starts one day prior to the starting date of the reference

345 track (starting on the 28th) follows the track until the 29th early hours (~~Figure 1g to i~~ Fig. 1i to n) when it diverges and ends up in North Africa, underlying a missed forecast. This is consistent also for earlier starting dates (the 25th and the 26th) with a greater error in terms of initial position (not shown). ~~Figure-Fig. 1~~ shows that, as expected, the simulations with initial conditions perturbations ~~present-usually~~ (INI and TOT) tend to show more spread in the initial position. However, the spread at later stages in the simulation seems to be similar for both the INI experiment and the two experiments with the ~~perturbation-on-the~~ physics-physics perturbation, SPP, and SPP-Conv, ~~while on the other hand, the TOT experiment shows a slightly higher spread~~ than the others simulations.

For Ianos the 16th of September was chosen as an example, but the behavior for the three starting dates is quite similar, with ~~them-being-able-to-reproduce-the-trajectory~~ the trajectory being reproduced quite well for the first days and the error increasing with time. The latter is ~~computed~~ calculated as the root mean ~~squared-square~~ error between the ensemble mean track and the reference track. It never exceeds 300 km (not shown) and ~~up-to-48-hours~~ is always below 100 km up to 48 hours (not shown). The error values are similar in all three experiments, but slightly lower for the INI and TOT experiment. In the case of Zorbas and Trixie, since the starting dates are earlier than ~~when-the-reference-track-starts~~ the start of the reference track, the earlier the simulations start, the ~~more-uncertainty-there-is-with-respect-to-the-starting-position,-thus-the-more-spread.~~ In Figure 1 the latest ~~starting-dates-simulations-are-shown-for-both~~ greater the uncertainty in the start position, and hence the greater the spread. Fig. 1 shows the latest simulated starting dates for all cyclones. For Zorbas, starting ~~from-on~~ on the 27th, the obtained tracks ~~are following-follow~~ the reference with a small error, at least for the first days, which is anyway always ~~under-below~~ under 300 km, ~~at in~~ later stages. As in the case of Ianos ~~the-error-committed-by-the-three-~~ the error made by the four experiments is similar. For Trixie, the error ~~regarding-the~~ goes up to 700/800 km for the four experiments with respect to the 27th, the last ~~starting-start~~ starting-start date shown in ~~Figure-figure 1g, hand-i,-goes-up-to-700/800-km-for-the-three-experiments,-and-i.~~

The tracking results shown in ~~Figure-Fig. 1~~ are mirrored by the ensemble spread and the relationship between the spread and the error presented in ~~Figure-2-and-Figure-Fig. 2 and Fig. 3~~ respectively. Following the approach of Hamill et al. (2011), the spread of the ensemble for a single cyclone ensemble forecast at a given forecast time is defined as:

$$370 \quad S_i(t) = \frac{1}{n} \sum_{i=1}^n D_i \quad (3)$$

where D_i denotes the great-circle distance of the i th ensemble member position of the cyclone from the ensemble mean cyclone position. The total number of ensemble members used for the calculation is 24 and the spread has been computed for each starting date (3 dates for each medicane). The results, reported in ~~Figure-2,-regard-the-same-starting-Fig.2,-are-for-the-same~~ start date as in ~~Figure-1,-thus-for-Ianos-the-16th-of-September,-for-Zorbas-the-27th-of-September,-and-for-Trixie-the-27th-of~~ October, as Fig. 1, i.e. 16 September for Ianos, 27 September for Zorbas, and 27 October for Trixie, which is also representative of the spread of the other ~~starting-start~~ dates. It is ~~shown-that-for-the-three-cyclones-the-INI-experiment-shows-found-that~~ the ~~TOT-experiment-has-the~~ largest mean track spread (Figure 2 a, b for the three cyclones (Fig.2 a), b) and c). Then the-, but is comparable to the INI ensemble for most of the simulation period. The spread for the SPP and ~~the-SPP-Conv~~ ensembles

spread is comparable, reaching similar values is comparable and lower than the other two experiments but reaches a similar value to the INI ensemble at the end of the simulation. Ianos and Zorbas present and Zorbas show less spread than Trixie upon initialization at initialization, especially for the INI experiment in particular. This might and TOT experiments (which are probably dominated by the initial perturbation at the beginning). This may be due to the fact that for Trixie, which whose analysis track starts on the 28th of October (Figure 28 October (Fig. 1g to 1i)) a great, there is a large uncertainty in the initial position of the track exists.

When looking at the spread-skill relationship (Figure 3), measured by the ratio of the ensemble spread and the root mean squared error between the ensemble mean track and the reference track, it can be said that as mentioned before the error is always greater than larger of the ensemble spread and they are only comparable in the first hours of the simulations (20h to 40h) when the spread/skill values are nearer to 1. Both the SPP and closer to one. The SPP, the SPP-Conv are usually and the INI are generally more under-dispersed than the INI-TOT experiment in all three cases, but the three experiments perform. The former three experiments behave generally in the same way, with the INI experiment presenting lower showing less error after the second day for Ianos and Zorbas, but behaving similarly in Trixie. for Trixie. The TOT experiment performs better for Zorbas, but not for Trixie and Ianos.

At later forecast steps, Trixie is the cyclone with the highest spread for all three perturbations compared to Ianos and Zorbas. By looking at the general spread trends, the INI while during the first two days of the simulations, the initial perturbations dominate the spread for all cases, by day 3 the spread from the physical parametrizations becomes equivalent. As a result the spread of the TOT ensemble, which is a combination of the two, tends to compare well with the INI ensemble at the beginning of the simulation and then to the SPP and SPP-Conv at later stages. The INI experiment spread is highest at initialization, as also seen in Lang et al. (2012), since the EDA perturbations (INI experiment) are associated with a shift and intensification/weakening of the cyclone. Even considering the case-to-case variability, in terms of the spread of the track, the SPP-Conv experiment is the one with consistently less spread for all the cyclones. The low error values obtained by Ianos and Zorbas, compared to the values reached those obtained in the case of Trixie (≥ 800 km), make it not only the medicane with the largest spread but also the the one with the most significant error. Indeed, it has been verified that this particular simulated cyclone diverges deviates from the analysis track. The Trixie simulation track is probably a result of the ensemble forecast not capturing properly the processes connected to the simulation track of Trixie is probably due to the fact that the ensemble forecast does not correctly capture the processes associated with cyclogenesis, but it can also be related to the simulations starting fact that the simulations start too early before the medicane appearance appearance of the medicane. This is an aspect also recognized by (Di Muzio et al., 2019) in the simulation of these events.

It has to be noted here, that both experiments with SPP Interestingly, both SPP experiments, and specifically the SPP-Conv one, manage to produce a spread comparable to the one produced by the initial condition perturbation, produce cyclone spread that is comparable at the later stages of the simulation to the experiment with initial condition perturbations only. Similar results have been found in Lang et al. (2012). These results underline the importance of the role of convection and convective heating in

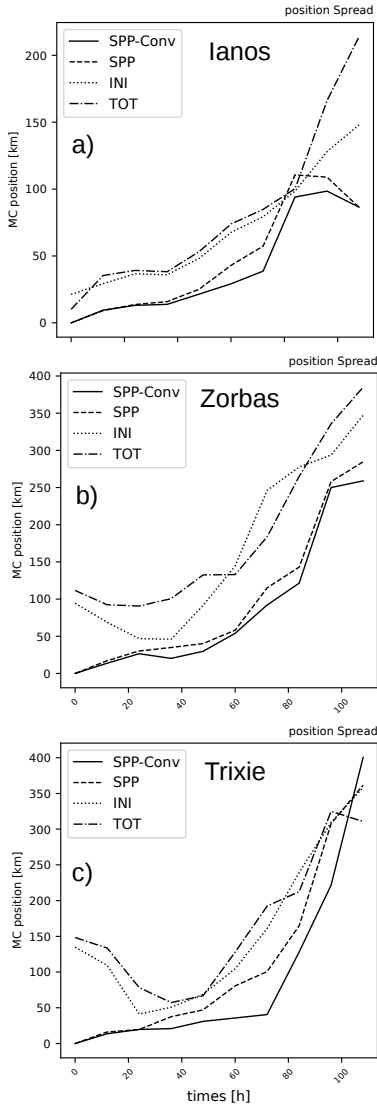


Figure 2. Mean ensemble spread of the medicanes track for each ensemble perturbation experiment for Ianos (a), Zorbas (b) and Trixie (c). The track spread is computed as described in Eq. 3 and is reported in km. For Ianos the experiments starting on the 16/09 have been chosen, for Zorbas the ones starting on the 27/09 and for Trixie the ones starting from the 27/10, in order to be consistent with the ensemble tracks shown in [Figure Fig. 1](#)

explaining the source, underlining the initial condition and physical heating-related sources of uncertainty in the development tracking of these cyclones.

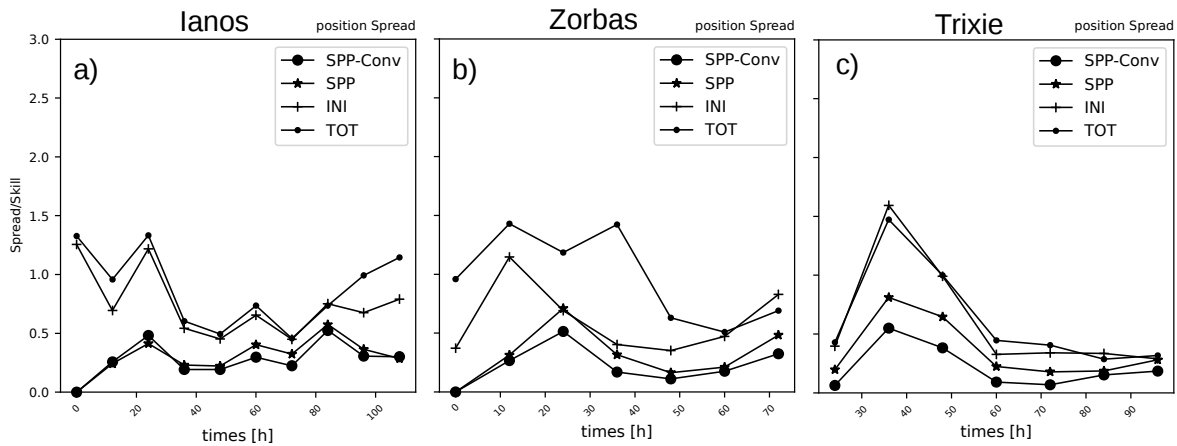


Figure 3. Ensemble Spread/skill relationship for each ensemble perturbation experiment for Ianos (a), Zorbas (b) and Trixie (c). The spread is computed as in Eq. 3 and the skill is the root mean squared error between the ensemble mean and the analysis tracks. For Ianos the experiments starting on the 16/09 have been chosen, for Zorbas the ones starting on the 27/09 and for Trixie the ones starting from the 27/10, in order to be consistent with the ensemble tracks shown in Figure 1.

415 4.2 Intensity

The other important aspect investigated is the intensity of the cyclones analyzed. The intensity is assessed by studying the minimum core pressure at the cyclone position.

The development of the core pressure with the simulations is reported in Figure Fig. 4 where the mean sea level pressure at the centre of the cyclone (Minimum Core Pressure in Figure Fig. 4) is shown, with the ensemble mean, the 25%-75% percentile and the 5%-95% percentile compared to the analysis for the three ensemble experiment for chosen starting dates, as an example. For Ianos there is an overestimation of the deepening-of-the-cyclone (Figure-cyclone deepening (Fig. 4a, d and g, g and l), with a temporal-time shift of one day, compared to the analysis, which is consistent in all three experiments. For Zorbas the minimum pressure is underestimated only in the case of the SPP-Conv experiment, however, there is a shift of 12 hours compared to the analysis in the three experiments (Figure-Fig. 4b, e and h, h and m). In the case of Trixie, there is an underestimation (Figure-Fig. 4c, f and i, i and n) and the ensemble experiments are not able to capture the entire-development full evolution of the cyclone pressure (especially the second deepening around the 30th).

In-For all three cyclones, the spread is slightly larger-higher for the SPP and the SPP-Conv experiment-experiments compared to the INI one, however, the TOT experiment is the one with the highest spread for the three cyclones. The reference analysis is included in the ensemble spread of the latter experiments (INI and TOT) compared to what happens with the SPP experiments, at least in the initial timestep-time steps. This is particularly true for Ianos (Figure-Fig. 4a, d and g, g and l). For Zorbas, the deepening-of-the-pressure-pressure deepening is slightly better captured by the SPP ensembles (Figure-4b and h and the TOT

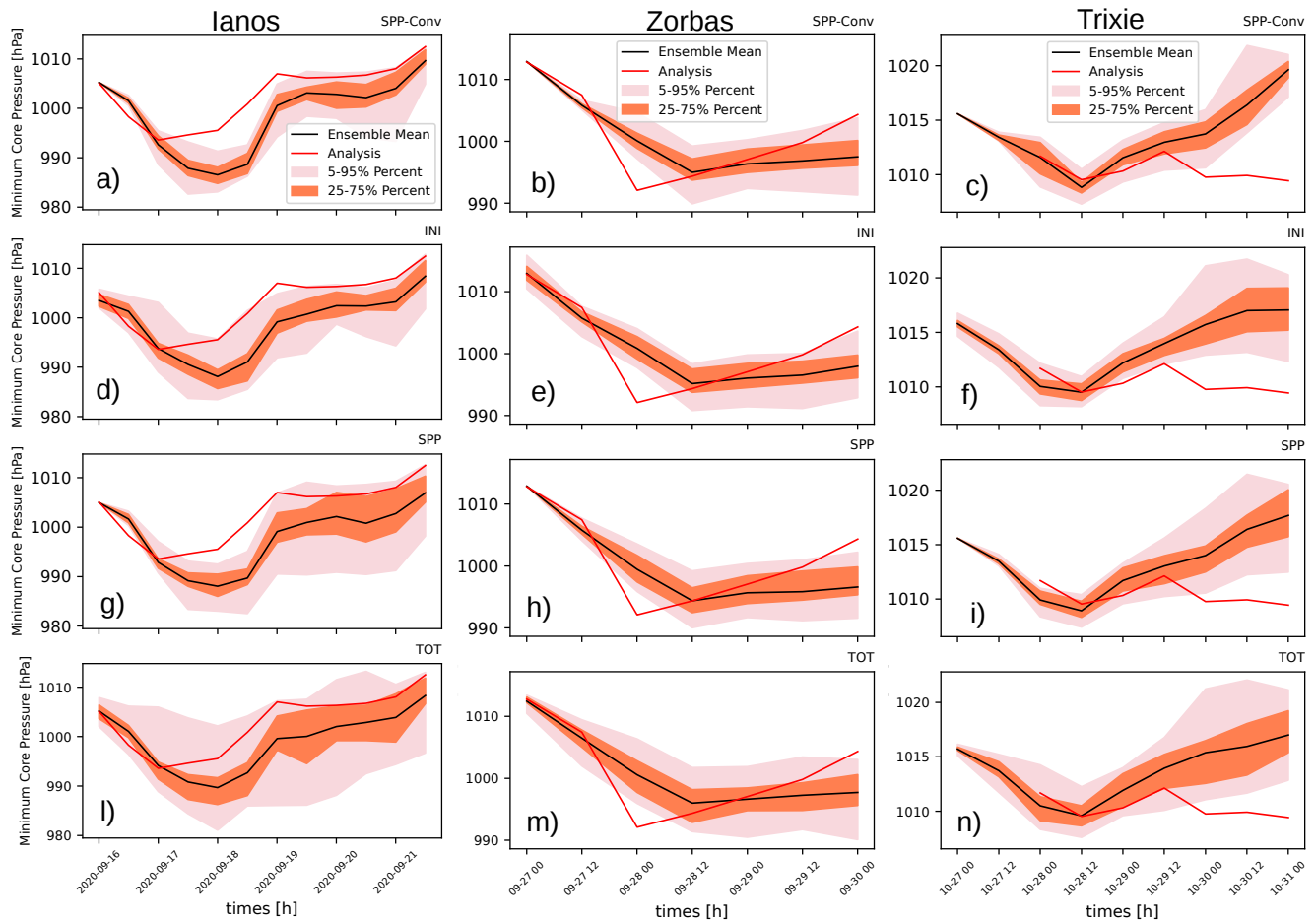


Figure 4. Analysis of the mean seal level central pressure, for Ianos in the first column, for Zorbas in the second column, and for Trixie in the third column. The plots show the ensemble members' development throughout the simulation. In each Figure Fig. the ensemble mean is reported in black, the operational analysis is reported in red and the two shaded areas represent the 25-75 % percentile and the 9-95 % percentile. The SPP-Conv experiment is reported for each medicane in Figures Fig. (a), (b), and (c). The INI experiment is reported in Figures Fig. (d), (e) and (f) and the SPP experiment in Figures Fig. (g), (h) and (i) in (b), and the SPP-TOT experiment in (e), (m), (n).

ensembles (Fig. 4b, h and m). As pointed out before, there is a shift of the minimum pressure of 12 to 24 hours compared to the analysis. For Ianos this is also present in the simulation starting on the 15th but is absent when starting the simulation in the simulation starting on the 17th. This is due to the improved initial conditions with the forecast start date when the forecast starts closer to the occurrence event. The same can be said for Zorbas. As for Trixie, besides For Trixie, apart from the first deepening happening on the 28th of October, which is well captured by all the experiments, the second minimum, which is the deepest, is not captured by any of the members of every experiment, even if starting from experiments ensemble members, even when starting on the 27th of October (the last starting start date). In general, there is an underestimation of the pressure

440 ~~minimum and the trend~~ minimum core pressure, and its evolution up to the 29th is captured better by the TOT experiment,
followed by the SPP experiment (Figure 4i). Fig. 4i and n). Overall, the TOT ensemble, the operational forecast at ECMWF,
performs better in terms of core pressure, since it includes both the initial perturbation and the model perturbation.

4.3 Precipitation

The precipitation field has also been analyzed and verified against observation. The verification field is chosen to be the precip-
445 itation, as in Vich et al. (2011); Montani et al. (2011). Matching the forecast ~~and with~~ the verifying data is ~~made difficult~~
~~hampered~~ by the irregularly spaced ground network of observations and by the ~~fact that precipitation is not a continuous~~
~~field, thus a point-to-point verification presents several problems and is guaranteed by using satellite data.~~ Thus, in this work
~~observations from satellites, specifically the above-discussed spatial variability of precipitation.~~ Therefore, satellite products,
in particular the above mentioned Integrated Multi-satellite Retrievals for GPM (GPM-IMERG), are used.

450

The precipitation structure of the three medicanes, in terms of intensity and position, is similar to what is observed in tropical
cyclones (Zhang et al., 2021, 2019). Indeed, there are similarities in their rainfall structures and those for Mediterranean
cyclones (Flaounas et al., 2018) where most precipitation associated with medicanes is concentrated to the northeast side of
the cyclone centre, as is shown in Figure 5 for the three cyclones. For the three ~~eyelone~~ cyclones, the ensemble mean of the
455 last starting date is shown. For each cyclone, the daily accumulation on the day of the "tropical-like" phase is shown in Figure
Fig. 5. For Ianos this is the 17th of September, for Zorbas is the 28th of September, and for Trixie is the 28th of October. The
daily accumulation values from the ensemble forecast experiments are comparable ~~, within the error~~ to the observed values
only regarding Ianos. In general, the maximum is better captured by the SPP experiments for Ianos (Figure Fig. 5a and c),
while for Zorbas and Trixie, this is true for the INI ~~and~~, the TOT and the SPP-Conv experiments (Figures 5e, f, i and Fig. 5f, g,
460 and i). The standard deviation of each ensemble experiment ~~reveals shows~~ that there is higher uncertainty ~~related to associated~~
~~with~~ the higher values of the precipitation distribution (Supplementary Figure Fig. S1). This is consistent for all three cyclones.
There is little difference between the SPP-Conv and the SPP experiment in terms of precipitation distribution. This mirrors
what was shown in Figure Fig. 4.

465 The positioning of the maximum precipitation in the presented distributions (Figure Fig. 5), ~~in general, is in accordance is~~
generally consistent with the observed GPM-IMERG distribution. However, there are some other secondary maximums in the
distribution that are not well captured, for all three cyclones. This is possibly related to the simulation resolution not being able
to capture completely the precipitation structure. Preliminary results from the recent work of the Destination Earth (DestinE)
project (Gascón et al., 2023) shows that the accumulated precipitation pattern is slightly better captured by the 4 km simulation
470 compared to the 9 km one with the IFS model (https://confluence.ecmwf.int/x/w53m for Ianos, reported as an example).

The daily accumulated precipitation shown in Figure Fig. 5 belongs to the simulations with the latest starting date, where the
maximum precipitation is better captured. Indeed, the error in the simulated ensemble mean precipitation maximum compared

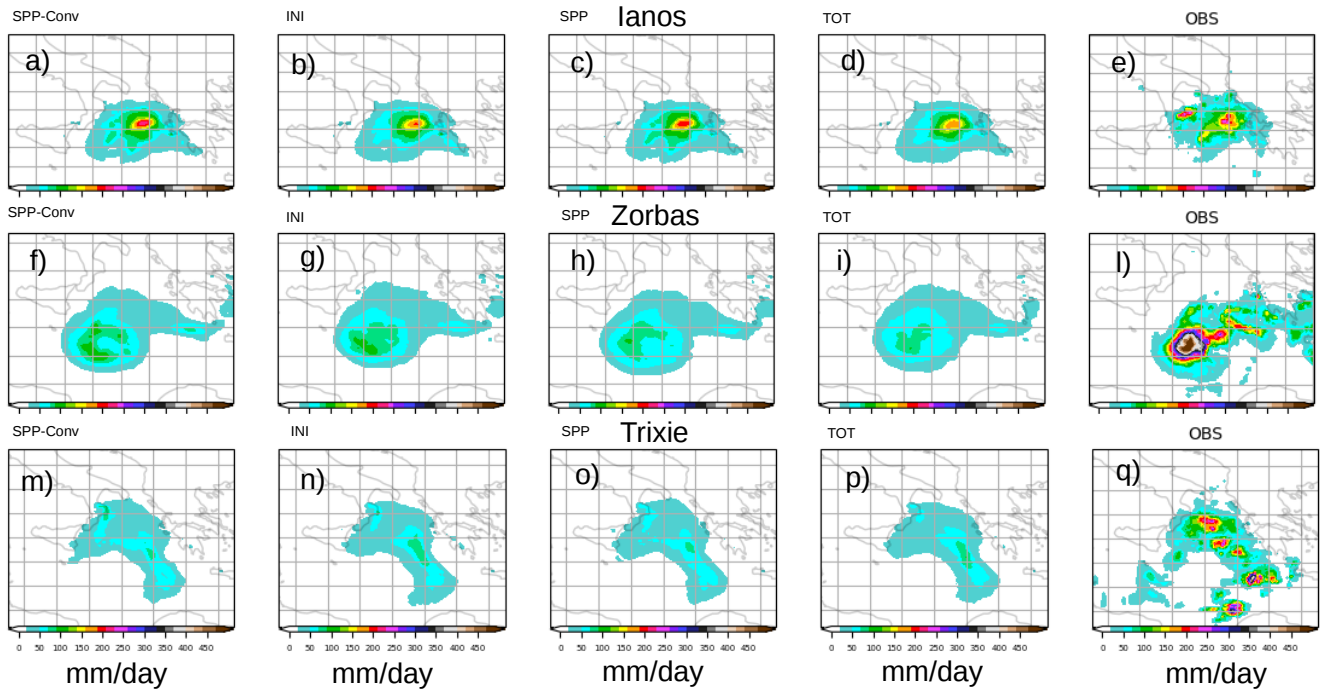


Figure 5. Daily accumulated precipitation (mm/day) for the three ensemble experiments ensemble means compared to the satellite observation GPM-IMERG. For Ianos the 17th is shown in [Figures Fig. \(a\), \(b\), \(c\) and \(d\) and \(e\)](#). For Zorbas the 28th is shown in [Figures Fig. \(ef\), \(fg\), \(gh\), \(i\) and \(hl\)](#). For Trixie the 28th is shown in [Figures Fig. \(im\), \(ln\), \(mo\), \(p\) and \(nq\)](#). ~~the The SPP-Conv ensemble forecast accumulated precipitation is reported in the first column, the SPP-INI ensemble in the second column, the INI-SPP ensemble in the third column, the TOT ensemble in the fourth column, and the observations in the fourth-fifth column.~~ For Ianos the experiments starting on the 17th ~~is are~~ shown, for Zorbas the ones starting on the 27th and for Trixie the ones starting from the 27th.

to the observation is decreasing with the forecast start date closer to the medicane occurrence. This is specifically true for Ianos and Zorbas (as ~~it is~~ shown in Supplementary [Figure Fig. S2](#)), while for Trixie, the maximum is ~~equally also~~ underestimated. For Trixie, the simulation is not able to capture the intensity of the precipitation. This is linked to the absence of the deepening of the cyclone and the precipitation starts to decrease sensibly after the 28th. This is seen within all the starting dates. ~~In order to evaluate the whole performance of the ensemble some probabilistic precipitation thresholds have been chosen from 1 to 150 mm, and all the ensemble members have been considered. Following the cyclone position at each timestep, an area of 500~~

475 ~~km² around the cyclone centre has been considered for evaluation. The analysis has been carried out using many verification measures, following the literature (Montani et al., 2011; ?; Vich et al., 2011; ?). A brief description of these measures is given in the Supplementary Information. All the verification results have been calculated for the entire simulation period, according to their starting date.~~

Starting with the Brier Score (BS) (?) it can be said that the three ensemble experiments for the three medicanes are generally

485 ~~better than the control forecast at simulating the observed precipitation at all thresholds, as it is shown in Figure ??.~~ Indeed, BS

indicates the root mean squared error between the observed and the forecast probabilities, thus the lower the better, and in our study, the BS is higher in the control run than in the three perturbations runs.

Brier score for the SPP-Conv ensemble forecast experiment, for the SPP ensemble forecast experiment, and for the INI ensemble experiment for Ianos (a), Zorbas (b) and Trixie (c).

490 For Ianos, which presents the lowest values, the three perturbation ensembles are almost indistinguishable (Figure ??a), while for both Zorbas and Trixie the perturbation experiment SPP-Conv has a slightly higher value than the SPP and the INI experiment (Figure ??b and ??c). The difference between the three experiments decreases with increasing thresholds, and in general, the improvement of the ensemble experiments compared to the control run decreases for extreme events when the Brier score tends to zero as the events become increasingly rare. To further analyze the respective skill of the three ensemble
 495 experiments, the Relative Operating Curve (ROC) has been computed as a measure of forecast resolution. In general, for precipitation from 2 to 50 mm the ROC reached values between 0.7 and 0.8 for Ianos and Zorbas (not shown) which indicates a useful forecast (?). The difficulties in predicting extreme precipitation, values over 50 mm may be probably due to the grid length of 9 km

500 In the fourth column of Fig. 5, the TOT ensemble means are shown. The latter ensemble mean compares well to the INI ensemble, similar to what happens for the standard deviation of each ensemble experiment (Supplementary Fig. S1 and S2), thus confirming the results of the tracking and intensity.

4.4 Thermal structure and asymmetry

To complete the analysis of these three storms, the thermal structure, and the thermal asymmetry have been investigated. The chosen parameter to quantify the latter has been recognized in the upper-level thermal wind The Hart parameters, $-V_T^U$, which
 505 is considered to be a relevant parameter in distinguishing tropical-like cyclones from fully baroclinic cyclones (Mazza et al., 2017), and secondly on the thermal asymmetry, B . These parameters belong to the theory of the three-dimensional cyclone phase space introduced by Hart (2003). There, the thermal asymmetry is defined as the storm-motion relative 900–600 hPa thickness asymmetry across the cyclone within its radius:

$$B = \frac{(\overline{Z_{600 \text{ hPa}} - Z_{900 \text{ hPa}}}|_R - \overline{Z_{600 \text{ hPa}} - Z_{900 \text{ hPa}}}|_L)}{}$$

510 where Z is the geopotential height, R indicates the right of current storm motion, L indicates the left of storm motion, and the overbar indicates the areal mean over a semicircle around the cyclone centre.

Instead, the cyclone's upper-level thermal structure (i.e., its cold or warm core) is indicated by $-V_T^U$. If it attains a positive sign, the cyclone attains an upper-level warm core. Indeed the $-V_T^U$ is defined as:

$$-|V_T^U| = \frac{\partial(\Delta Z)_{300 \text{ hPa}}}{\partial \ln(p)_{600 \text{ hPa}}}$$

515 The two pressure levels have been changed from 600 hPa to 700 hPa and from 300 hPa to 400 hPa due to the lower height of the tropopause in the midlatitudes with respect to the tropics (Picornell et al., 2014). These values are computed within

a 200 km radius around the detected cyclone center. In the Hart (2003) formulation, this radius was chosen to be 500 km, but given the smaller size of medicanes compared to tropical cyclones (Miglietta et al., 2013), the radius used in this study is smaller, 200 km. The choice to consider important only the upper-level structure, compared to the lower-level (thus using also the lower-level thermal wind $-V_T^L$) is because its positive value can characterize not only medicanes but also extratropical cyclones with warm occlusion (Hart, 2003). In the case of the thermal asymmetry, the threshold value of $B = 10 \text{ m}$ has been determined by analyzing ECMWF reanalyses ERA40 at 1.125° of the resolution, from which no major hurricane (winds of greater than 210 km/h) had associated with it a value of B that exceeded 10 m (Hart and Evans, 2001). Even if the threshold value of B has been originally determined for larger tropical/extratropical cyclones, previous studies have shown that such value is also useful in the case of medicanes (Miglietta et al., 2011).

The Hart parameters, $-V_T^L$ and B , are analyzed in Figure 6. The focus has been put on the values where the deepening of the cyclone occurred in the observation, thus the values in Table 2 are reported as references in Figure 6. The violin plots of the forecast distribution for each experiment at different starting dates are shown with the median (white dot) and the interquartile range (gray bar). The sections at the sides of each violin plot represent the kernel density estimation to show the distribution shape of the data (wider sections of the violin plot represent a higher probability that members of the population will take on the given value; the skinnier thinner sections represent a lower probability). The choice for the violin plot has been made because, unlike a box plot that can only show summary statistics, violin plots depict summary statistics and the density of each variable. In Figure 6 only the SPP-Conv and the INI experiments are shown for comparison, because the results of the SPP experiments, as already pointed out above, are very similar to the one those obtained by the SPP-Conv.

The forecast distribution in the three ensemble experiments presents different behaviors compared with the analysis reference value (ref in Figures 6) and with the starting date in the three experiments. Generally, the three ensemble experiments can reproduce the thermal structure of the storms, showing in some cases decreased a reduced spread with forecast start date closer to the occurrence, probably linked related to the fact that these starting dates coincide with the period in which the cyclone had already developed (see Figures 6a and c for Ianos) and that the appearance of a symmetrical storm can benefit from improved initial conditions Di Muzio et al. (2019) (Di Muzio et al., 2019). This behavior is consistent for all three perturbation experiments.

The simulations of Ianos show a reduced spread with later starting dates accompanied by the distribution value approaching the analysis value, for the thermal wind (Figures 6a and c), and the thermal asymmetry (Figures 6b and d). Specifically, for the thermal asymmetry B , this makes the spread of the ensemble to be included below the threshold of 10 m which would define the system as a frontal system rather than a non-frontal one (Miglietta et al., 2013), thus showing a better performance in reproducing the tropical-like phase of medicanes. This is true for both experiments, INI and SPP-Conv, and also as well as for Zorbas and Trixie. In the case of Zorbas, there is a usually

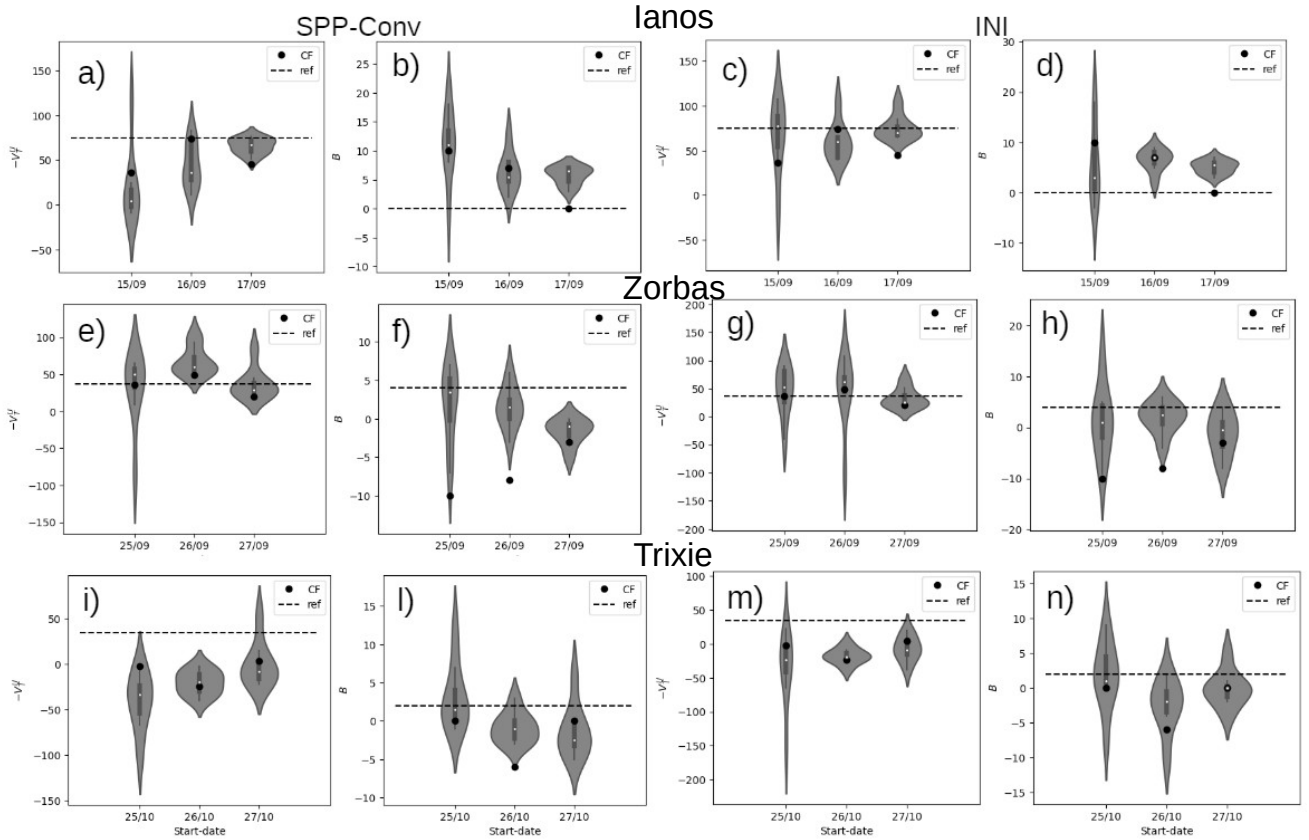


Figure 6. Ensemble forecasts violin plots of thermal wind, $-V_T^U$, and thermal symmetry, B , for each starting date for Ianos in [Figures-Fig. \(a\) and \(b\)](#) for the SPP-Conv ensemble forecast and in [Figures-Fig. \(c\) and \(d\)](#) for the INI ensemble forecast, for Zorbas in [Figures-Fig. \(e\) and \(f\)](#) for the SPP-Conv ensemble forecast and in [Figures-Fig. \(g\) and \(h\)](#) for the INI ensemble forecast and for Trixie in [Figures-Fig. \(i\) and \(l\)](#) for the SPP-Conv ensemble forecast and in [Figures-Fig. \(m\) and \(n\)](#) for the INI ensemble forecast. The violin plot is a hybrid of a box plot and a kernel density plot, which shows peaks in the data. The white dot represents the median, the thick gray bar in the center represents the interquartile range (25th-75th) and the thin gray line represents the rest of the distribution. On each side of the gray line is a kernel density estimation to show the distribution shape of the data.

smaller spread for the last starting date only regarding the thermal wind ([Figures-Fig. 6e and g](#)). Instead, there is a comparable spread for the thermal asymmetry, especially [regarding for](#) the INI experiment ([Figure-Fig. 6h](#)). However, the forecast distribution of both experiments contains the reference analysis values for both the thermal wind and the thermal asymmetry ([Figure Fig. 6e to h](#)). In Trixie, the spread is comparable between the starting dates for the thermal asymmetry parameter and thermal wind ([Figures-Fig. 6i to n](#)). There is [also](#) a consistent underestimation of the thermal wind (with median values of $-V_T^U$ around -25 to -50), in all three ensemble experiments. The forecast distribution is closer to the analysis values ($-V_T^U = 39$) for the third starting date, for both ensemble experiments, as shown in [Figures-Fig. 6i and m](#). This underestimation of the upper-level

thermal wind means that a warm core was never reached in the ensemble forecast experiments, as it will be explored in the following sections.

4.5 Tropical-like phase

A more in-depth analysis of the

5 Results: Physical processes analysis

To understand the processes of cyclone formation, intensification and tropical-like phase of these Mediterranean cyclones is carried out by means of the divergence (s^{-1}), vorticity (s^{-1}), and time tendencies of the temperature (K/s) and specific humidity ($g/kg/s$) profiles around the cyclone centre (within a radius of 200 km). The latter profiles are reported in Figure 8 to 10 for the SPP-Conv experiment as an example and in there the temperature and humidity tendency are reported as Q1 for temperature and Q2 for humidity as is usual in the literature (Grabowski et al., 1999; Yanai et al., 1973), where $Q1 = \frac{dT}{dt}$ and $Q2 = -\frac{L_v}{c_p} \frac{dq}{dt}$. For data volume phase and how they affect the forecast, a comparison was made between the operational analysis and the ensembles. To reduce the amount of data, the analysis of the ensembles has been was reduced to consider a subset of 8 members, instead of 24. In the case of Ianos, which becomes a warm core cyclone on the 17th of September (Figure 8c and d at 00 UTC), the Q1 signals that the warming is happening at 500 hPa and it has deepened from 12 hours earlier, on the 16th of September (Figure 8a at 12 UTC), where the maximum is located at 600 hPa. This indicates a deepening warm core. Q2 signals the presence of diabatic heating by condensation throughout the mid-troposphere, which is increasing in the tropical phase. The tropical-like phase is accompanied by strong divergence above 400 hPa and convergence below 800 hPa (Figure 8b and d). The vorticity increases in the mid and upper troposphere on the 17th (Figure 8d) compared to the 12 hours prior. The warm core is sustained for another day and the cyclone starts disappearing around the 19th. By the 20th (Figure 8e and f) the cyclone is dying out, with almost no divergence and no convective warming. Analysis of the intensification and transition to tropical-like characteristics for Ianos as represented by the SPP-Conv experiment. The $Q1 = \frac{dT}{dt}$ and $Q2 = -\frac{L_v}{c_p} \frac{dq}{dt}$ profiles are shown in the first column and the vorticity and divergence profiles are shown in the second column. Figures (a) and (b) are taken on the 16th of September at 1200 UTC. Figures (c) and (d) are taken on the 17th of September at 0000 UTC. Figures (e) and (f) are taken on the 20th of September at 1200 UTC. These profiles belong to the simulation starting on the 16th.

Similar behavior can be observed for Zorbas in Figure 9. The divergence increases above 400 hPa in the tropical phase, around the 28th of September (Figure 9d at 12 UTC) compared to the previous day (Figure 9a and b on the 27th at 12 UTC). The same can be said for the vorticity in the upper and mid-troposphere. The warming intensifies and moves to the upper troposphere (Q1 and Q2 profiles in Figure 9a and c). After two days of "tropicalization" the cyclones starts to weaken and by the 1st of October (Figure 9e and f) the divergence is almost null and the warming is decreased. The results obtained here resemble the ones obtained also for tropical cyclones (Geetha and Balachandran, 2016; Lin and Qian, 2019) while intensification is occurring. For this reason, it can be said that Ianos and Zorbas actually undergo a tropical phase. There,

the heating that is observed in the simulation is caused by the release of latent heat in the condensation process inside clouds, as also confirmed by observations for Ianos (Zimbo et al., 2022).

595 Same as Figure 8 but for Zorbas. Figures (a) and (b) are taken on the 27th of September at 1200 UTC. Figures (c) and (d) are taken on the 28th of September at 1200 UTC. Figures (e) and (f) are taken on the 1st of October at 1200 UTC. These profiles belong to the simulation starting on the 27th.

For Trixie instead, the warm core state is never reached. As said before this cyclone is the weakest and it can intensify only on the 28th in the ensemble simulations (Figure 10c and d at 00 UTC). The convective heating represented by a positive Q1 and Q2 is weaker compared to the other cyclones (Figure 8 and 9) and the maximum is located in the mid-troposphere, signaling a shallow warm core. The divergence, which is increasing compared to the previous 12 hours (Figure 10b and d) is 600 not accompanied by an increase in vorticity and it starts at mid-troposphere. In general, this phase, which does not correspond to a warm core, mirroring the results shown in Figure 6, is reached only in the 28th, but on the 30th, when Trixie is supposed to become a tropical-like cyclone (Dafis et al., 2020), is absent. The profiles regarding the latter day are shown in Figure 10e and f. The warming is weak and there is no divergence.

605 Same as Figure 8 but for Trixie. Figures (a) and (b) are taken on the 27th of October at 1200 UTC. Figures (c) and (d) are taken on the 28th of October at 0000 UTC. Figures (e) and (f) are taken on the 30th of October at 1200 UTC. These profiles belong to the simulation starting on the 27th.

By comparing Figure 8e, Figure 9e and Figure 10e it can be said that the spread is lower for Ianos, meaning lower uncertainty on the nature of the medicanne compared to Trixie and Zorbas. The spread in Zorbas is reduced by forecast start date closer to occurrence (not shown) in favor of the higher values for Q1 and Q2 (shown in Figure 9e which represents the profiles of the 610 latest starting date) mirroring Figure 6c and g. Trixie presents the highest spread regarding the warming, mirroring the results of Figure 6e to 6n.

These results indicate that Ianos and Zorbas are simulated mostly with the right tropical-like phase, with almost the right timing, while the ensemble simulation for Trixie fails to reproduce the right intensification of the cyclone, simulating a shallow warm core on the 28th and missing the deepening on the 30th.

615 **6 Process behind the intensification of the cyclone**

To understand the obtained results concerning the tropical-like phase and the development of the three cyclones, the focus is put on the simulation of the precursor events leading up to the medicanes formation and on the simulation and role played by convective instability and surface forcing for these cyclones.

5.1 Dynamical forcing and Potential Vorticity analysis

620 A crucial factor for the formation of intense Mediterranean cyclones is the

5.1 Cyclones formation

The synoptic environment favoring cyclogenesis in the Mediterranean is the presence of a deep upper tropospheric trough, cut off from the large-scale circulation and intruding into the Mediterranean. The latter can bring thermodynamic disequilibrium, owing to its deep cold air (Emanuel, 2005; Flaounas et al., 2022). As the low approaches the Mediterranean environment with small baroclinicity, the air masses are lifted, decreasing the temperature above and increasing convective instability. The presence of an intrusion of very cold air in the upper troposphere may allow for the conversion from thermal energy into kinetic one (Palmen, 1948). This is usually accompanied by the presence of air masses with high potential vorticity (PV) to intrude-intruding in the Mediterranean region (Flaounas et al., 2022), which usually triggers instability also in the case of extra-tropical cyclones (Flaounas et al., 2015; Raveh-Rubin and Flaounas, 2017). This stratospheric air mass is able to can introduce anomalous high PV in the upper troposphere, which induces thermodynamic instability strengthening the surface vortex below. Usually, this stratospheric air mass intrusion is called PV streamer (Claud et al., 2010) and it is evidenced here that it is present in all three medicanes. This is underlined in Figure 7 Fig. 7a to c for the operational analysis in which the height of the isosurfaces of 2 PVU ($\text{PVU} = \text{m}^2 \text{Kkg}^{-1} \text{s}^{-1} 10^{-6}$) is shown in relation to the mean sea level pressure for the three medicanes. When the PV anomaly can detach from the streamer then it continues to sustain the medicane in- These factors have already been found to be an integral part of Ianos and Zorbas formation in the literature, while for Trixie, to the tropical-like phase. This is what happens in the case of Ianos (Figure 7a) and Zorbas- authors knowledge, these aspects have never been fully analyzed. For Ianos, on 16 September the cut-off low was present (clearly identified at the 500-hPa level in Supplementary Fig. S3) and the PV streamer approached the area over the low center and wrapped around it (not shown), as also evidenced in Lagouvardos et al. (2022). Then, on 17 September, as it is shown in Fig. 7a the PV streamer broke up, resulting in the formation of a PV cutoff. Similarly, the formation of a PV streamer with the cutoff low already present (Supplementary Fig. S3) on 27 September over the Mediterranean was followed by cyclogenesis of Zorbas at the PV southeastern flank (Portmann et al., 2020) as it is shown in Fig. 7b, followed by a PV cutoff (not shown for the analysis but reported in Supplementary Figure Fig. S6 for the ensemble experiments). For Trixie, the presence of a cutoff low on 28 October (Supplementary Fig. S3) is accompanied by the PV streamer reaching the area in which the cyclone is forming, even if the interaction between the PV streamer and the cyclone is not so evident (Fig. 7c). However, it is noted here that the PV cutoff is never reached (reported in Supplementary Fig. S6 for the ensemble experiments).

The For Ianos in general, the PV streamer is well reproduced by the SPP-Conv and the other ensembles (not shown), especially regarding its interaction with the heating at 500 hPa (colored lines in Fig. 7d). However, on the 17th of September at 00 UTC the PV streamer detachment from the large-scale hasn't happened yet in Figure ??-, as Fig. 7d shows, but it will happen 12 to 24 hours later (Supplementary Figure Fig. S6) which is in line with what is shown in Figure Fig. 4 regarding the simulated minimum central pressure reaching the lowest value with a delay compared to the analysis. Nonetheless for Ianos, if This delay means that both in the analysis and the ensembles the medicane reaches its maximum intensity with the creation of the PV-cutoff, meaning that the former is dictated by the latter, at least for the timing. If starting from the 17th, the three ensembles are capable of reproducing can reproduce the PV cut-off from the large scale at the right timing. The PV streamer is well reproduced, especially regarding its interaction with the (not shown) probably due to initial conditions being closer

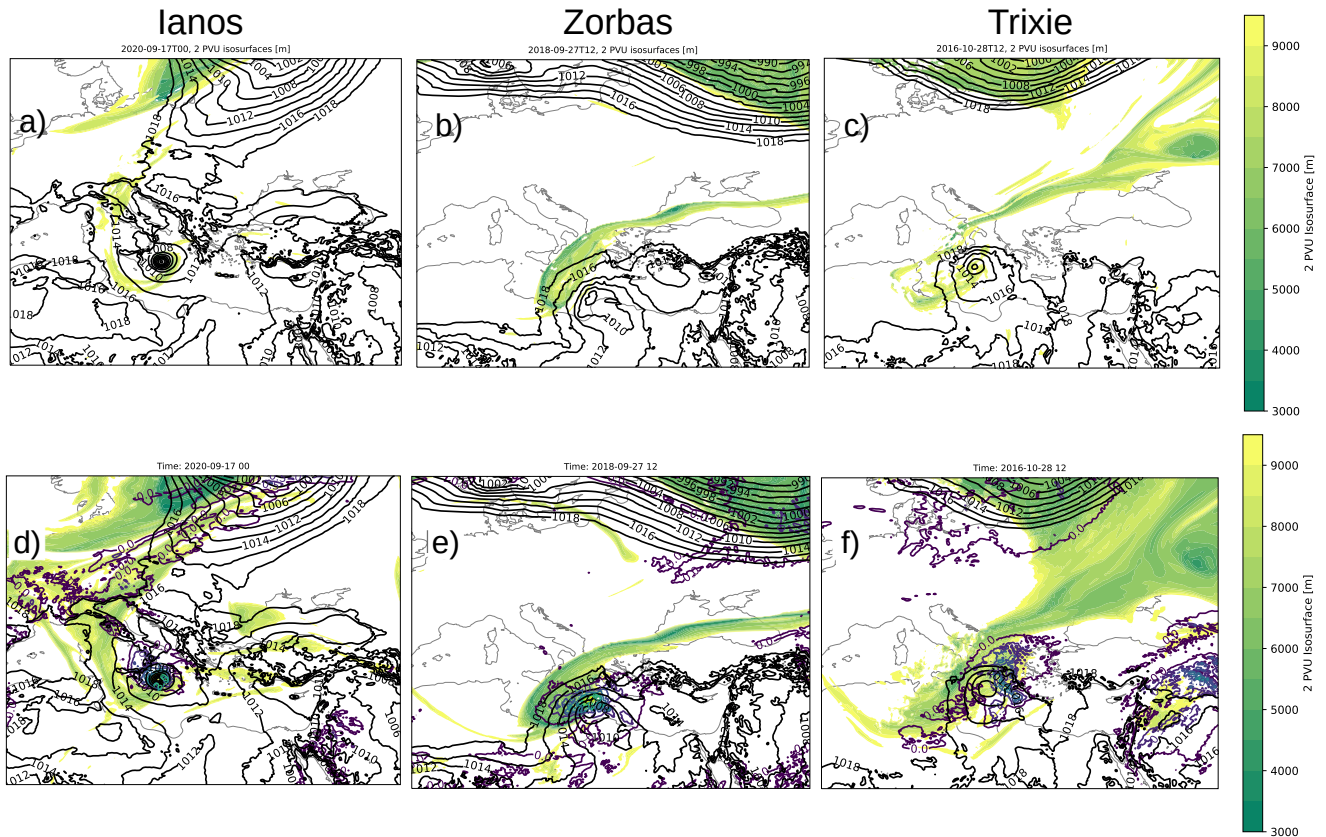


Figure 7. Height of the 2 PVU ($\text{PVU} = m^2 K kg^{-1} s^{-1} 10^{-6}$) isosurfaces together with the mean sea level pressure (black lines) in the operational analysis. For Ianos the 17th at 00 UTC is reported in Fig. (a) in the operational analysis and in (d) for the SPP-Conv ensemble experiment ensemble mean, for Zorbas the 27th at 12 UTC is reported in Fig. (b) in the operational analysis and in (e) for the SPP-Conv ensemble experiment ensemble mean and for Trixie the 28th at 12 UTC is reported in Fig. (c) in the operational analysis and in (f) for the SPP-Conv ensemble experiment ensemble mean. For Ianos the reported Fig. (d) is from the ensemble starting from the 17th, for Zorbas the reported Fig. (e) is from the ensemble starting from the 26th and for Trixie the reported Fig. (f) is from the ensemble starting from the 26th.

660 to the tropical-like conditions. When looking at the ensemble performance, a more in-depth analysis is carried out using the divergence (s^{-1}), vorticity (s^{-1}), and time tendencies of the temperature (K/s) and specific humidity ($g/kg/s$) profiles around the cyclone centre (within a radius of 200 km). The latter profiles are reported in Fig. 8 to 10 for the SPP-Conv experiment and in there the temperature and humidity tendency are reported as Q1 heating at and Q2 for temperature and humidity respectively, as is usual in the literature (Grabowski et al., 1999; Yanai et al., 1973), where $Q1 = \frac{dT}{dt}$ and $Q2 = -\frac{L_v}{c_p} \frac{dq}{dt}$, with Q1 representing the heating in Fig. 7. In the case of Ianos, which becomes a warm core cyclone on the 17th of September (Fig. 8c and d at 00 UTC), the Q1 signals that the warming is happening at 500 hPa (colored lines in Figure ??a) and it has deepened from 12 hours earlier, on the 16th of September (Fig. 8a at 12 UTC), where the maximum is located at 600 hPa.

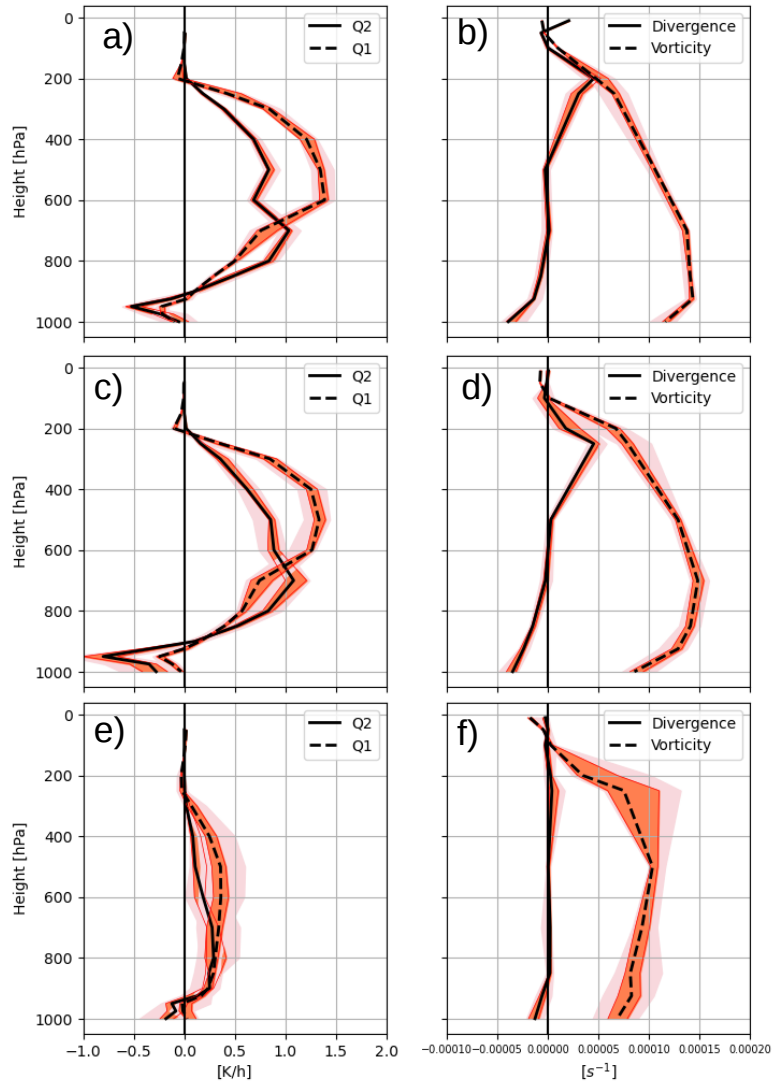


Figure 8. Analysis of the intensification and transition to tropical-like characteristics for Ianos as represented by the SPP-Conv experiment. The $Q1 = \frac{dT}{dt}$ and $Q2 = -\frac{L_w}{c_p} \frac{dq}{dt}$ profiles are shown in the first column and the vorticity and divergence profiles are shown in the second column. Fig. (a) and (b) are taken on the 16th of September at 1200 UTC. Fig. (c) and (d) are taken on the 17th of September at 00 UTC. Fig. (e) and (f) are taken on the 20th of September at 12 UTC. These profiles belong to the simulation starting on the 16th. The colours shading is the same of Fig. 4.

665 For Zorbas, the PV streamer is evident and it is occurring one day prior to the tropical phase (Figure Fig. 7b) thus inducing an intensification of the cyclone. This is well reproduced by the SPP-Conv ensemble experiment shown in Figure ??b Fig. 7e, as well as for the other two ensemble simulations INI and SPP (not shown). The values of the height of the 2 PVU isosurfaces

coincide between the operational analysis (in Fig. 7a to c) and the ensemble simulations (in Fig. 7d to f). Similar behaviour to the one seen in Ianos, regarding the heating, can be observed for Zorbas in Fig. 9a and b. On the 27th of September at 12 UTC the heating is below 600 hPa even if there is already a weak divergence over 600, underlining the presence of a still shallow vortex. Once again the PV-cutoff will happen 12 hours later when Zorbas will also reach the maximum intensity as indicated by Fig. 4 where a similar delay of 12 hours is present.

Regarding Trixie, the interaction between the PV streamer and the cyclone is not so evident (Figure 7e), but is reaching the area in which the cyclone is forming. Moreover, the In the case of Trixie, even if the PV anomaly is well reproduced by the SPP-Conv ensemble, compared to the analysis, the convective heating, reported in Figure ??e Fig. 7f, is not aligned with the PV streamer. This happens in the timestep time step where the cyclone is intensifying before dying out in the ensemble simulations (between 28 and 29 October). When looking at the vertical profiles in Fig. 10a and b, one day prior to 28 October, little warming (low values of Q1 and Q2 in the mid-troposphere) and low convergence in the lower troposphere can be noticed, lower values compared to the other two cyclones, nonetheless signaling a brief intensification phase for the cyclones. Indeed, when comparing these results with the minimum core pressure reported in Fig. 4 one can say that Trixie's initial state is well captured by the ensemble starting on the 27th leading to the first cyclone intensification of the 28th. However, if looking at the 28th). In Figure ??e the ensemble mean regarding the simulation starting from the 26th is shown, while for the ensemble mean of the other starting dates, in particular the 25th in specific, the PV streamer and the surface vortex are further even more misaligned. Indeed, with the forecast start starting date closer to occurrence the alignment the event, the alignment between the convective heating and the PV streamer is better reproduced (see Supplementary Figure Fig. S6). This has played a role in the missing intensification and tropical phase of the cyclones which also leads to a better reproduction of the cyclone intensity.

Height of the 2 PVU ($PVU = m^2 K kg^{-1} s^{-1} 10^{-6}$) isosurfaces together with the mean sea level pressure (black lines) and Q1 at 500 hPa for the SPP-Conv ensemble experiment ensemble mean. For Ianos the 17th at 00 UTC is reported in Figure (a) as simulated by the experiment starting from the 17th, for Zorbas the 27th at 12 UTC is reported in Figure (b) as simulated by the experiment starting from the 26th and for Trixie the 28th at 12 UTC is reported in Figure (c) as simulated by the experiment starting from the 26th.

Indeed, a Furthermore, while for Ianos and Zorbas, the presence of the cut-off low is well simulated by the ensemble experiments compared to the analysis (Supplementary Figs. S3 and S4), this is not the case for Trixie. In the ensemble simulations of Trixie, the cut-off low disappears after the 29th (Supplementary Fig. S5 shows the different reproduction of the presence of the cut-off low and how it changes with different starting dates). Its position and intensity had an influence on the track and intensity of Trixie, in accordance with what was suggested in the literature (Pytharoulis et al., 2000). Indeed, in the analysis, two distinct lows are formed separately (Supplementary Fig. S3) and the first to form is the one responsible for the Trixie surface vortex, by bringing instability from the upper troposphere to the lower troposphere. In the ensembles, this separation is not well captured. The formation of the second cut-off low prevails and the first one is weakened (Supplementary Fig. S4), influencing the development of Trixie after its formation, as will be discussed in the following section.

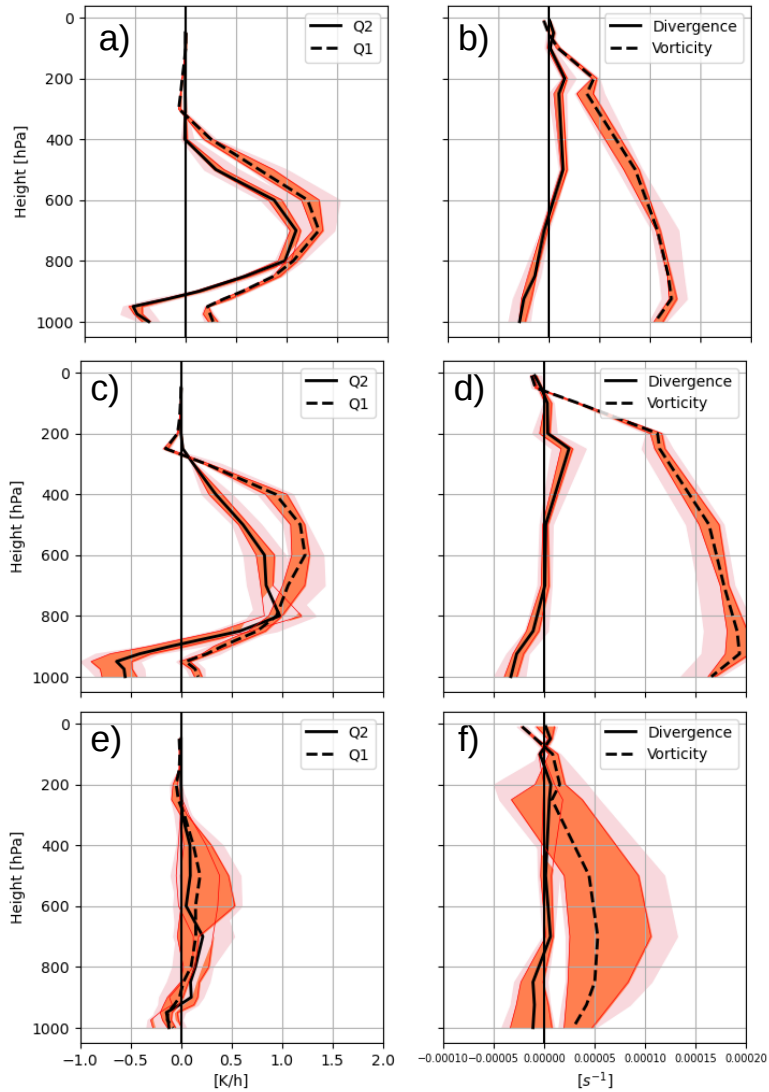


Figure 9. Height of the 2-PVU Same as Fig. 8 but for Zorbas. Fig. (a) isosurfaces together with the mean sea level pressure and (black lines b) in are taken on the operational analysis. For Ianos the 17th-27 September at 00-1200 UTC is reported in Figure. Fig. (ac) for Zorbas and (d) are taken on the 27th-28 September at 12-1200 UTC is reported in Figure. Fig. (be) and for Trixie (f) are taken on the 28th-1st of October at 12-1200 UTC. These profiles belong to the simulation starting on the 27th. The colours shading is reported in Figure (e) the same of Fig. 4.

5.2 Cyclones Intensification

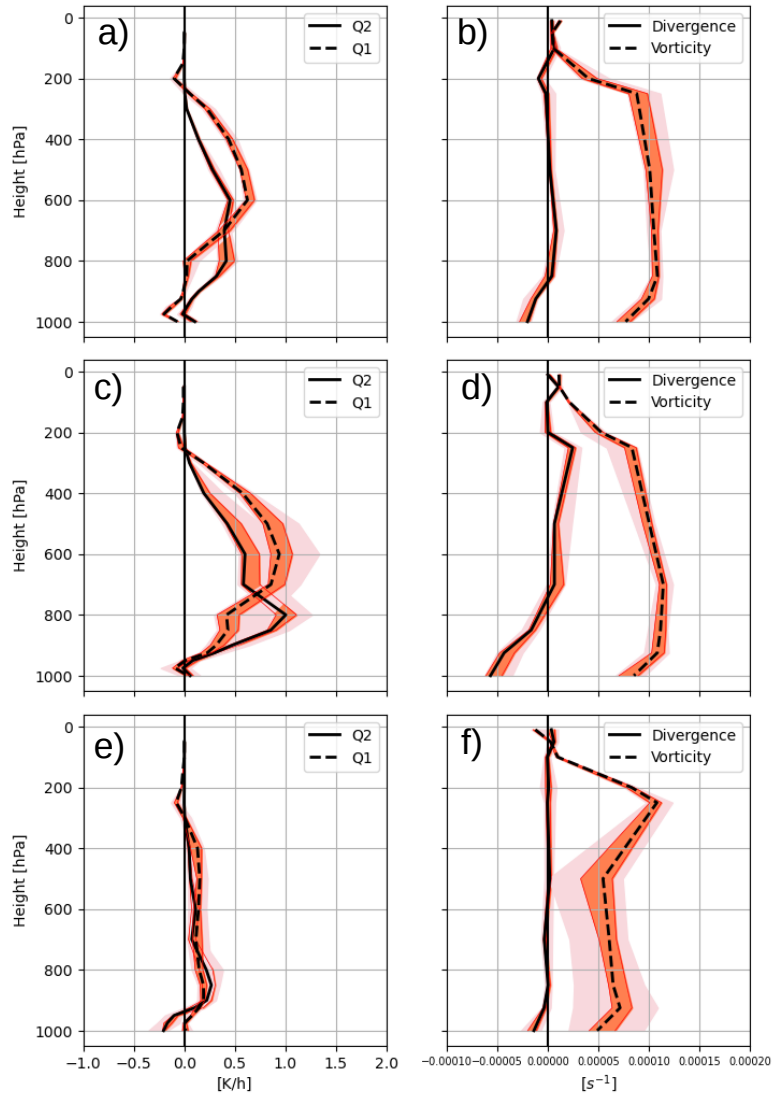


Figure 10. Same as Fig. 8 but for Trixie. Fig. (a) and (b) are taken on the 27 October at 1200 UTC. Fig. (c) and (d) are taken on the 28 October at 0000 UTC. Fig. (e) and (f) are taken on the 30 October at 1200 UTC. These profiles belong to the simulation starting on the 27th. The colours shading is the same of Fig. 4.

As underlined in the literature the factor that contributes to the evolution-development and intensification to reach a tropical-
 705 like state for Mediterranean cyclones is the pairing of the upper-level instability with the lower-level one. Carrió et al. (2017) underlined (Flaounas et al., 2022). More specifically, Carrió et al. (2017) highlights the importance of the upper-level dynamics in intensifying the surface vortex and supporting the tropical transition of the cyclone. This is what is shown in Figure shown in Fig. 11, which represents the potential vorticity field and the meridional and zonal winds in a cross-section of

latitude and pressure, at different stages for each medicane for the operational analysis. There, in ~~Figure Fig.~~ 11 a, d, and
710 g, ~~is present the PV field is shown for the 24 hours before the cyclone became tropical-like and it is shown that there is~~
an anomaly of ~~the~~ potential vorticity in the lower troposphere, around 800 hPa, which is a signal ~~of for~~ the formation of
a surface vortex for all the cyclones accompanied by a production of PV by diabatic processes. ~~This is happening in the~~
~~surrounding of the cyclone position. There, the PV field is shown for the 24 hours before the cyclone became tropical-like~~
715 ~~In~~ Flaounas et al. (2022), it is summarized that the processes that can underlie the lower-level PV maxima can be the surface
fluxes and the release of latent heat due to the organization of strong convective activity. In the upper troposphere, ~~an anomaly~~
~~of PV is developing and intruding a PV anomaly develops and penetrates~~ from the stratosphere. ~~This happens around the~~
~~position of the cyclone.~~ After 12 hours (~~Figure Fig.~~ 11b, e, and h) the two ~~anomalies of PV~~ PV anomalies, the upper and
~~the lower, the upper-level and the lower-level,~~ start to align. The same mechanism has been recognized in the literature by
~~Cioni et al. (2018); Miglietta et al. (2017)~~ Cioni et al. (2018) and Miglietta et al. (2017). Finally, the tropical phase is reached
720 when a cyclonic wind circulation completely ~~wraps around surrounds~~ the PV anomaly (~~Figure 11e~~ Fig. 11c, f and i):

~~, the so-called "PV-tower". This is the case for all three cyclones. However, for Zorbas and Trixie deep, convective activity~~
~~is higher during the intensification phase of the cyclone and then decreases as the maximum intensity is reached, as also~~
~~recognized by Dafis et al. (2020). This can be seen in the cross-sections reported in Fig. 11 where the lower level PV anomaly~~
~~is larger in the earlier stages before maximum intensity in Zorbas and Trixie (Fig. 11e and h) compared to Ianos (Fig. 11b). It~~
725 ~~should be noted that the generation of the diabatic PV anomaly in the lower and middle troposphere is relevant. In fact, as also~~
~~shown in the previous section, the alignment of the convective heating (taken at 500 hPa in Fig. 7d to f) and the PV anomaly is~~
~~necessary for the intensification of the cyclones.~~

~~In the simulation of these cyclones, the ensemble experiments behave similarly.~~ For Ianos, the tropical-like phase on the 17th
of September (~~Figure 12a and b) is reproduced quite nicely~~ is reproduced, with the INI experiment ~~presenting showing a~~ slightly
730 weaker PV than the SPP-Conv ensemble mean (for the simulation starting from the 16th shown in the ~~Figure~~ Fig. 12a and b).
~~The tropical-like phase is accompanied by strong divergence above 400 hPa and convergence below 800 hPa (Fig. 8b and d)~~
~~and by an increase of diabatic heating (Q2 profile) due to condensation. Vorticity increases in the middle and upper troposphere~~
~~on 17 September (Fig. 8d) compared to the 12 hours before. The warm core is sustained for another day and the cyclone begins~~
~~to dissipate around 19 September. By the 20th of September (Fig. 8e and f) the cyclone is dying out, with almost no divergence~~
735 ~~and no convective heating. Comparing Fig. 8c, Fig. 9c and Fig. 10c it can be said that the spread is smaller for Ianos, which~~
~~means less uncertainty about the nature of the medicane compared to Trixie and Zorbas. Moreover, in the case of Ianos, these~~
~~results compare well with the precipitation field shown in Fig. 5, which is the best simulated among the three medicanes, at~~
~~least regarding the simulations starting on the 17th. In addition, as mentioned in the analysis of the Hart parameters for Ianos,~~
~~the presence of a deep warm core is well simulated with decreasing spread and error with starting dates closer to the event~~
740 (Fig. 6a to d), correlating with the better reproduction of the PV-tower generation. The comparison between the SPP-Conv and
~~the INI ensemble shows that the former experiment produced a slightly more intense cyclone than the analysis and the latter~~
~~experiment, probably due to the effects of the convective parameterization perturbation.~~

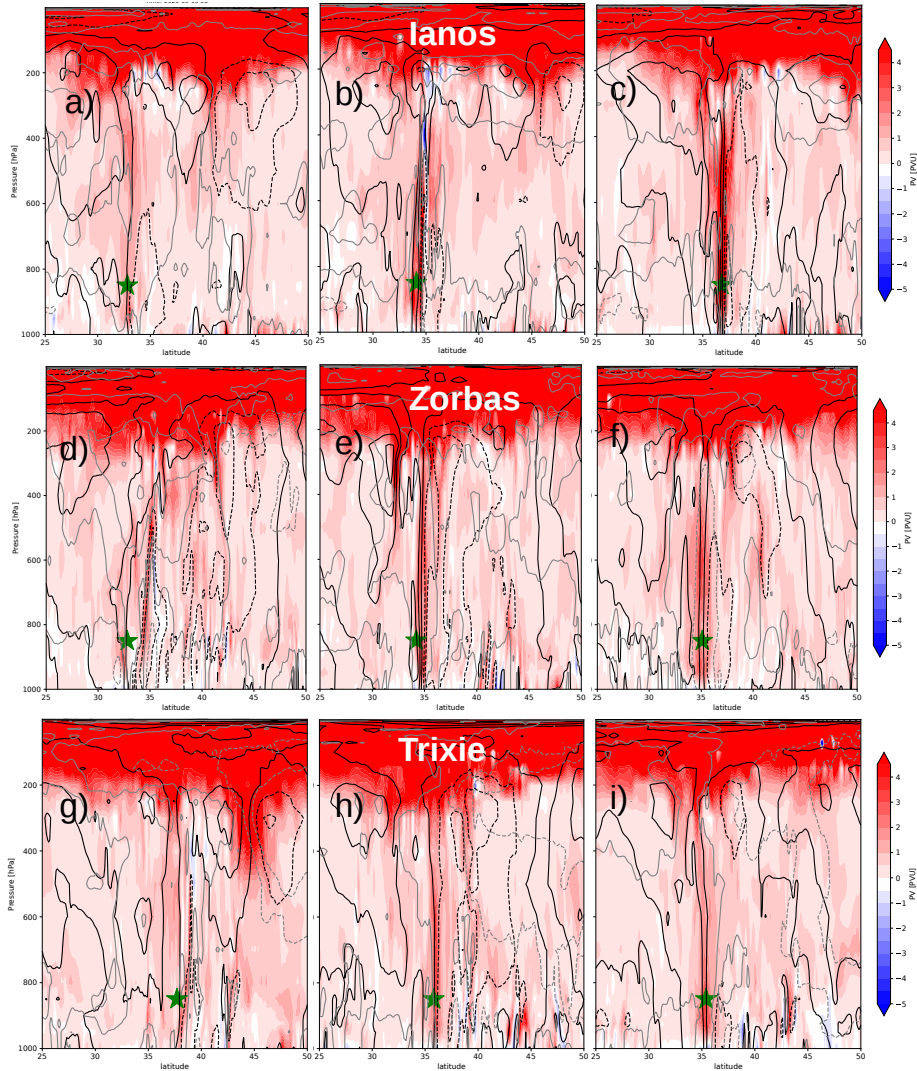


Figure 11. Operational cross section of the operational analysis Potential potential vorticity field cross-section in latitude at latitudes from 25° to 50° and pressure taken in \rightarrow at the longitude of the cyclone's central minimum pressure of the cyclones (green star). The PV is in colour and the black lines represent the zonal wind, while the gray grey lines represent the meridional wind. For Ianos the cross sections shown regard are for the 16th at 00 UTC, the 16-16th at 12 UTC and the 17th at 00 UTC in Figures Fig. (a), (b) and (c) respectively. For Zorbas the cross sections belong to the 27h-27th at 12 UTC, the 28th at 00 UTC and the 28th at 12 UTC in Figures Fig. (d), (e) and (f) respectively. For Trixie the cross sections belong to the 29h at 00 UTC, the 29th at 12 UTC and the 30th at 00 UTC in Figures Fig. (g), (h) and (i) respectively.

For Zorbas, on the 28th of September, the PV values in the two ensemble experiments are were higher than the analysis, signaling a slightly more symmetrical-symmetric and intense cyclone (Figure Fig. 12c and d), also in agreement with the

745

750 results for the Hart parameters shown in Fig. 6e to h. However, the two experiment ensemble ~~mean is very similar~~ means (INI and SPP) are very similar and they both represent the actual presence of a PV-tower. Looking at Zorbas vertical profiles in Fig. 9, it can be seen that the divergence increases above 400 hPa in the tropical phase, around 28th September (Fig. 9d at 12 UTC) compared to the previous day (Fig. 9a and b on the 27th September at 12 UTC). The same is true for the vorticity in the upper and middle troposphere. The warming intensifies and moves into the upper troposphere (Q1 and Q2 profiles in Fig. 9a and c). After two days of "tropicalization" the cyclones begin to weaken and by the 1st of October (Fig. 9e and f) the divergence is almost null and the warming decreases. These results obtained for Ianos and Zorbas are similar to those obtained for tropical cyclones (Geetha and Balachandran, 2016; Lin and Qian, 2019) where intensification occurs. Therefore, it can be said that Ianos and Zorbas go through a tropical phase in the ensemble experiments. There, the heating observed in the simulation is 755 caused by the release of latent heat in the condensation process inside the clouds, as also confirmed by observations for Ianos (Zimbo et al., 2022; Lagouvardos et al., 2022). Indeed, heat fluxes from the sea surface often trigger convection and support intense and persistent diabatic warming through latent heat release from condensation (Carrió et al., 2017). As shown below, the surface fluxes played a role in the intense phase of both Zorbas and Ianos. The spread in Zorbas is reduced by the forecast start date closer to the event (not shown) in favour of the higher values for Q1 and Q2 (shown in Fig. 9c which represents 760 the profiles of the latest start date) which justifies the results for the Hart parameters in Fig. 6e to h. Here, the spread of the upper-level thermal wind is reduced and the error decreases.

~~Trixie instead, as mentioned above~~

~~Trixie, on the other hand,~~ does not present enough strong surface vortex to ~~align with match~~ the PV anomaly in the upper level for both experiments (Figure Fig. 12e and f) ~~for starting on the 25th as the starting date. If one looks into.~~ Looking at 765 the other starting dates ~~simulation it appears that there is simulations, there appears to be~~ a stronger lower-level instability (not shown).

~~However, this cannot be sustained by the simulation.~~

~~Thus, the occurrence of a strong surface-level vortex is prevented in the Trixie simulations (Figure 12). This is firstly due to the fact that the alignment of the surface vortex PV production and the~~ For Trixie indeed, the deep warm core state is never 770 reached. As said before this cyclone is the weakest and it can intensify only on the 28th of October in the ensemble simulations (Fig. 10c and d at 00 UTC). The convective heating represented by a positive Q1 and Q2 is weaker compared to the other cyclones (Fig. 8 and 9) and the maximum is located in the mid-troposphere, signaling a shallow warm core. The divergence, which is increasing compared to the previous 12 hours (Fig. 10b and d) is not accompanied by an increase in vorticity and it starts at mid-troposphere. The warming is weak and there is no divergence (Fig. 10e and f). Trixie presents the highest spread 775 regarding the warming, also mirroring the results from the Hart parameters reported in Fig. 6i to n. The warming, which does not correspond to a shallow warm core, is reached only on the 28th of October but is absent on the 30th of October, when Trixie is supposed to become a tropical-like cyclone (Dafis et al., 2020). Thus the Hart parameters values are justified by the absence of upper-level PV ~~is not well reproduced. Furthermore, it has to be pointed out that in the ensemble simulations, there is the absence of a strong cut-off low (deep upper tropospheric trough, cut off from the large-scale circulation), a precursor event that sustains the medicane Emanuel (2005) (Supplementary Figure S5 shows the different reproduction of the cut-off~~ 780

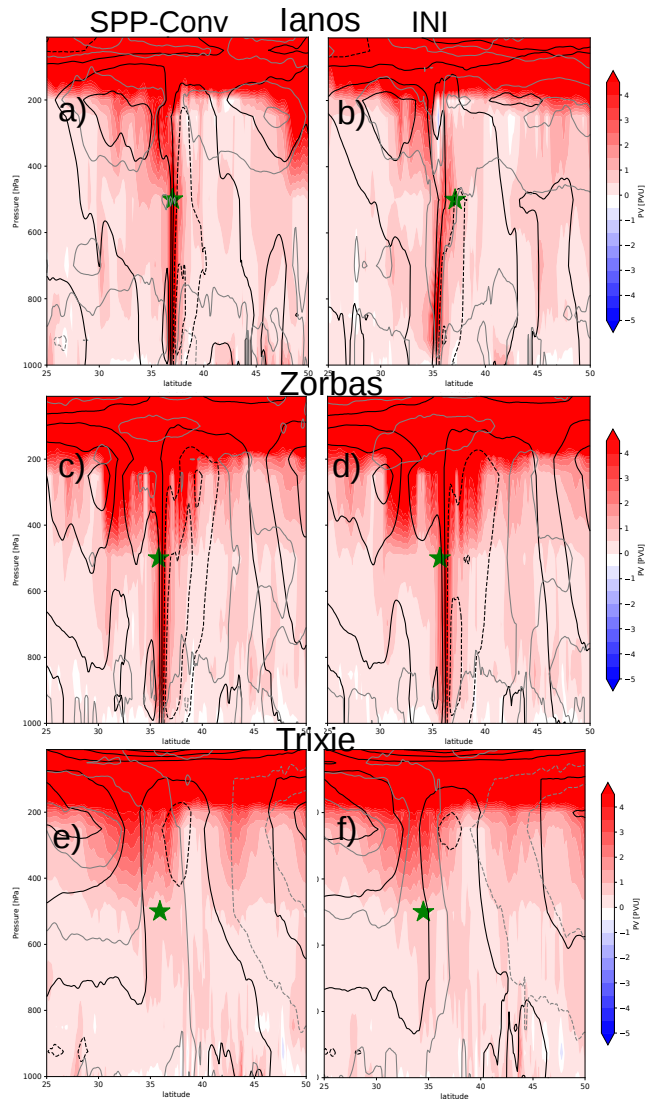


Figure 12. Potential vorticity field cross-section in latitude from 25° to 50° and pressure taken in the longitude of the central minimum pressure of the cyclones (green star) as represented by the SPP-Conv and the INI ensemble means in the first and second column respectively. The PV is in colour and the black lines represent the zonal wind, while the gray lines represent the meridional wind. For Ianos the cross sections shown regard the 17th at 00 UTC in [Figures Fig. \(a\)](#) and [\(b\)](#). For Zorbas the cross sections belong to the 28th at 12 UTC in [Figures Fig. \(c\)](#) and [\(d\)](#). For Trixie the 30th at 00 UTC is shown in [Figures Fig. \(e\)](#) and [\(f\)](#) respectively.

low presence and how it changes with different starting dates). The cut-off low position and intensity have had an influence on the tracking and intensity of Trixie, in accordance with what was suggested in the literature Emanuel (2005). Indeed, in the analysis, there are two distinct lows that form (supplementary Figure S3), and [warming for Trixie](#). This is also correlated

785 with the minimum core pressure development presented in Fig. 4 and for the accumulated precipitation in Fig. 5, where every ensemble experiment diverges from the analysis and observations after the 29th of October. These results indicate that Ianos and Zorbas are simulated mostly with the right tropical-like phase, with almost the right timing (12 to 24 hr of delay as mentioned above), while the ensemble simulation for Trixie fails to reproduce the right intensification of the cyclone, simulating a shallow warm core on the first one is responsible for the Trixie surface vortex, by bringing instability from the upper troposphere to the lower troposphere. Instead, in the ensemble simulations the formation of the second cut-off low prevails and the first one is weakened (Supplementary Figure S4). With the weakening of the cut-off low, Trixie starts lowering its intensity (around the 29th). Only a few members are able to follow the weak cut-off low (Supplementary Figure S3). This has had an impact on the simulation of the already weak cyclone that is Trixie. Indeed, Trixie is in general weaker than the other two cyclones (the central minimum pressure of Trixie is higher than the other two cyclones, as reported in Table 2), thus there is a chance that this fact has influenced the ensemble simulations. To investigate these aspects the focus is put on some other elements involved in the development of Trixie

790 28th and missing the deepening on the 30th.

795

5.3 Convective Instability and surface forcing

First of all, the The ensembles appear to have been able to better reproduce the large-scale upper-level dynamics, but there seem to have been issues in reproducing the presence or absence of PV anomalies generated by diabatic processes and the latter interaction with the upper-level one, specifically for Trixie. In order to understand this latter aspect, the convective activity in the three medicanes has first been analyzed by means of the Convective Available Potential Energy (CAPE)

800 has been analyzed for the three medicanes and specifically for Trixie, showing. The main result is weaker convection indicated by a weaker CAPE in Trixie. Indeed in Figure Fig. 13 there is a comparison between CAPE around the cyclone centre for Zorbas and Trixie at the intensification tropical-like state. The In the ensembles, the reduced convective activity reported in

805 Figure near the centre reported in Fig. 13 for Trixie underlines the lower energy production due to diabatic heating in Trixie ensembles simulations conversion from diabatic heating. Such a situation can be ineffective to drive in driving the cyclone to a state in which it is able to self-sustain by the wind-induced surface fluxes (Emanuel, 1986) and the transition to the tropical-like cyclone being degraded as already found in Koseki et al. (2021).

810 This is correlated with the effect of the surface fluxes, being much higher in the case of Zorbas and Ianos compared to Trixie (Supplementary Figure Fig. S7). By the Indeed, also the total heat flux at the surface (the sum of the sensible and latent heat flux) has been inspected. In Supplementary Fig. S7 is made clear that in the ensembles for Ianos and Zorbas the surface fluxes amount to around 500 W/m^2 and are concentrated for Ianos around the centre and for Zorbas are much more spread out. For Trixie, instead, the values are much lower and not at all comparable with the other cyclones. In general, by the 29th of October,

815 in the Trixie simulation, the convection is weakening and by the 30th is absent in the ensemble experiments, compared to the analysis. Thus, this reduced CAPE in the ensemble simulations is signaling a simulated weaker low-level vortex and a lower

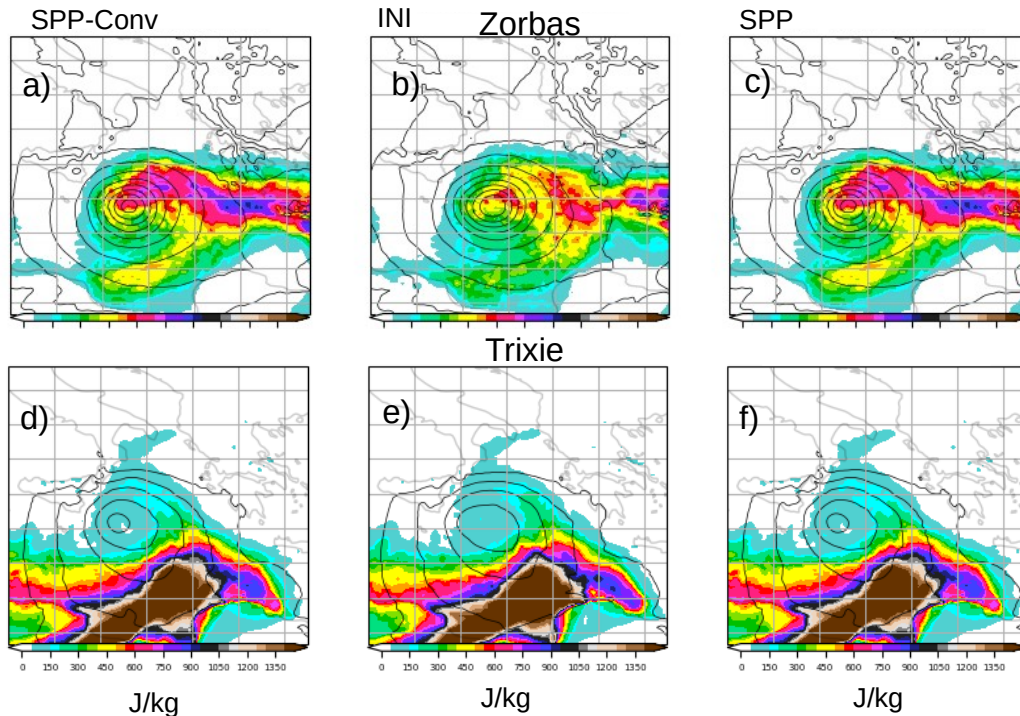


Figure 13. Convective Available Potential Energy (J/kg) (in colours) and mean sea level pressure (in lines) for the three ensemble experiments ensemble means. For Zorbas the 28th at 12 UTC is shown in Fig. (a), (b) and (c) for the simulation starting from the 27th. For Trixie the 28th at 12 UTC is shown in Fig. (d) (e) and (f) for the simulation starting from the 27th.

PV anomaly.

820 Convective Available Potential Energy (J/kg) (in colours) and mean sea level pressure (in lines) for the three ensemble experiments ensemble means. For Zorbas the 28th at 12 UTC is shown in Figures (a), (b) and (c) for the simulation starting from the 27th. For Trixie the 28th at 12 UTC is shown in Figures (d) (e) and (f) for the simulation starting from the 27th. The surface level production of PV in Trixie is not enough to match with the upper tropospheric high PV field as reported in Fig. 12e and f, or they are not in phase. In the ensemble simulations starting on the 27th, the amount of diabatically generated PV comparable to the analysis is not able to align with the upper-level one, even though the alignment is better captured with starting dates

825 closer to occurrence (Supplementary Fig. S6). This pertains to both the INI and SPP experiments, as mentioned before, meaning that the production of the right diabatic processes is equally sensitive to initial conditions and to physical and more specifically convective processes. The analysis points out that the cyclone dies before the 30th of October, due to the low-level vortex being too weak and not able to interact properly with the upper-level disturbances. Actually, the surface vortex disappears with the weakening of the upper-level cut-off low, and due to the absence of a reinforcement of the lower level PV production by the

830 upper level one, meaning erosion of PV by the presence of intense diabatic processes, as for instance is happening in Zorbas

(Portmann et al., 2020). Firstly, as mentioned in the previous Section, in the ensemble simulations of Trixie (both INI and SPP), the cut-off low that was crucial for the formation of the surface cyclone, disappears after the 29th and the formation of the second cut-off low weakens the first. With the weakening of the cut-off low, Trixie starts lowering its intensity. Only a few members can follow the weak cut-off low (Supplementary Fig. S3). This has had an impact on the simulation of the already
835 weak cyclone, Trixie. Indeed, it is hypothesized that Trixie is formed as a lower-level vortex mainly due to the thermodynamic disequilibrium generated by the upper-level cut-off low. If the latter is not well simulated, being weaker, it is not able to sustain the surface vortex. Secondly, when the surface level vortex is better reproduced, the misalignment with the upper-level PV anomaly does not permit reinforcement of the convection. Homar et al. (2003); Cioni et al. (2018) showed that the upper-level PV structure indirectly acts on the cyclone deepening through a modification of the surface circulation.

840

As mentioned above, the simulation of strong convective activity seems to be important in all three cyclones, which is associated with latent heat release, developing in the central region of the cyclones (Fig. 8, 9 and 10). As recognized in the literature, either the surface fluxes or convective activity can predominate in the intensification of the surface level vortex, as identified for different medicanes (Davolio et al., 2009; Miglietta et al., 2017; Chaboureau et al., 2012; Fita and Flaounas, 2018)
845 . While surface fluxes seem to have also played a role in the intensification of both Ianos and Zorbas (Supplementary Fig. S7), in the case of Trixie specifically deep moist convection seems to be the main mechanism leading to the maintenance and deepening of the system, as due to the interaction of convection with the upward forcing induced by the PV streamer (Chaboureau et al., 2012). Indeed, for Trixie is the long-lasting deep convective activity that may have played an important role in their intensification later than their genesis time, as also recognized by Dafis et al. (2020), and its weakening or even
850 absence compromises the forecast, as happens in the presented ensemble experiments. While the tracking is mainly influenced by the position of the cutoff low and the PV streamer position, the simulation intensification phase and timing are dependent on how the convection is reproduced and interacts with the upper-level PV structure.

5.3 The role of the Sea Surface Temperature

By looking at the Sea Surface Temperature (SST) anomaly, it is found that it is higher for Zorbas (Ianos is once again similarly
855 affected by the SST anomaly as Zorbas) upon formation compared to Trixie, as reported in ~~Figure 14 which is showing Fig. 14 which represents~~ the ensemble mean anomaly of the SPP-Conv and INI experiments for Zorbas and Trixie for comparison. ~~There, it is shown that if on~~ On one hand, for Zorbas (~~Figure Fig. 14a b and c~~) the SST is anomalously high compared to the climatological SST of September (obtained by using the ERA5 reanalysis SSTs over the Mediterranean Basin from 1991 to 2020), of on average ~~2°~~, ~~for Trixie~~ ° C. On the other hand for Trixie, the anomaly (with respect to the climatological SST of
860 October) decreases, and in the area of cyclone formation is very weak compared to Zorbas (~~Figure Fig. 14d, e and f~~). This means that the air-sea temperature contrast did not play a crucial role in Trixie generation and maintenance as it did for Ianos and Zorbas, probably resulting in weaker low-level vortex altogether ~~(mirroring what is shown in Supplementary Fig. S7 for the surface fluxes)~~.

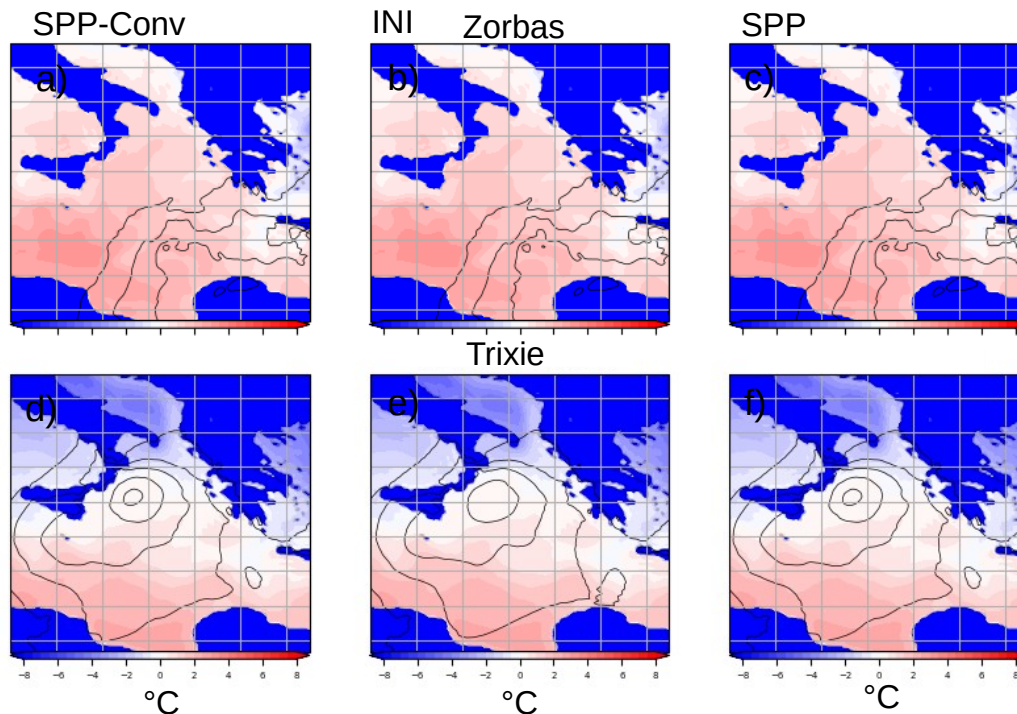


Figure 14. Sea surface Temperature anomaly ($^{\circ}\text{C}$) (in colours) and mean sea level pressure (in lines) for the three ensemble experiments ensemble means. For Zorbas the 27th at 00 UTC is shown in Figures Fig. (a), (b) and (c) for the simulation starting from the 27th. For Trixie the 28th at 00 UTC is shown in Figures Fig. (d) (e) and (f) for the simulation starting from the 27th.

865 Indeed, the ensemble experiments results compare fairly well to the operational analysis for the SST anomaly for the three medicanes (not shown), underlining the relative importance of the air-sea interaction in the tropicalization of the certain Mediterranean cyclones. The higher surface temperatures in Ianos and Zorbas help feed the medicane the moisture, through surface fluxes (Pytharoulis, 2018), allowing the convection to develop more effectively (Koseki et al., 2021; Cioni et al., 2018). Thus, it is evinced that Zorbas and Ianos tropical-like phase is also sustained by diabatic processes, while Trixie is not.

870 Indeed, it is hypothesized that Trixie is formed as a lower-level vortex mainly due to the thermodynamic disequilibrium generated by the upper-level cut-off low. Thus, if the latter is not well simulated, being weaker, it is not able to sustain the surface vortex. In turn, the surface level production of PV is not enough to match with the upper tropospheric high PV field as in Figure 12e and f. There, the convective-generated PV is not strong enough or not able to align with the upper-level one. Indeed, the interaction between the two latter, the convectively produced PV at low levels, and the PV streamer aloft has been deemed to be crucial for the development of the Mediterranean cyclones (Cioni et al., 2018).

875

The intensification of the cyclone is better captured by increasing the starting date (as it is shown in Supplementary Figure S6), because with forecast start date closer to occurrence the alignment is better reproduced and also there is more low-level PV production. However, the cyclone still dies before the 30th of October, due to the low-level vortex being too weak that is

not able to interact properly with the upper-level disturbances. Indeed in the operational analysis, it is evident that after the
880 29th the upper-tropospheric perturbation is cut off from the large scale, resembling what is happening in the case of Ianos
and Zorbas (Figure ??b), while this is isn't the case in the ensemble experiments. There the surface vortex disappears with
the weakening of the upper-level cut-off low, and due to the absence of a reinforcement of the lower-level PV production by
Noyelle et al. (2019) found that the upper-level one-

Homar et al. (2003) showed that the SST state has a strong influence on the medicanes intensities and that increased SSTs
885 lead to greater probabilities of tropical transitions, stronger upper-level PV structure indirectly acts on the cyclone deepening
through a modification of the surface circulation. Thus, it is very likely that the modification of PV in the simulations affects the
forecast of the trajectory and of the intensity, when the alignment of the upper-level PV and of the lower-level one is absent.
Furthermore, a fact that seems to be important in all three cyclones is the simulation of strong convective activity, which is
associated with latent heat release, developing in the central region of the cyclones (Figure 8, 9 and 10). Indeed is deep moist
890 convection that is the main mechanism leading to the maintenance and deepening of the system (Cioni et al., 2016, 2018; Flaounas et al., 20
, and its weakening or even absence compromises the forecast. The simulation intensification phase and timing are probably
dependent on how the convection is reproduced. In Trixie, the starting dates are probably too early to reproduce the right
convective activity to sustain the cyclone.

To conclude, the right positioning of the PV streamer in the intensification of these types of Mediterranean cyclones had been
895 recognized by Portmann et al. (2020). There they applied it to one of the medicanes here studied, Zorbas. In their study, they
reported that the correct, PV streamer position resulted in the most accurate forecasts with a strong medicane in most members,
up to three days prior to intensification. In this study, this is the right temporal range to observe a good forecast for Zorbas
and Ianos, while for Trixie one can clearly see how this uncertainty is affecting the forecast warm cores and lower pressure
minimum pressure, by influencing the intensity of fluxes from the sea, which leads to greater convective activity before the
900 storms reach their maturity. The higher surface temperatures in Ianos and Zorbas help feed the medicane the moisture, through
surface fluxes (Pytharoulis, 2018), allowing the convection to develop more effectively (Koseki et al., 2021; Cioni et al., 2018)

6 Discussion and Conclusion

Predicting and simulating medicanes is a difficult task due to them being extreme events found near the tail of the forecast distri-
905 bution (Majumdar and Torn, 2014) and due to the complexity of the processes involved. The specific barriers to predictability
and the atmospheric conditions that lead to medicanes the formation and evolution of medicanes are not fully understood.
Research utilizing using multi-physics approaches has found that the track, intensity, and duration of medicanes are heavily
sensitive to factors such as convection, microphysics, and boundary-layer parameterizations (Ragone et al., 2018; Miglietta
et al., 2015). This study indeed is a first step towards the understanding of Indeed, this study is one of the first steps toward
910 understanding this sensitivity by using ensemble forecast simulation.

The analysis ~~has been~~ was focused on three medicanes ~~with the use of the~~ using the ECMWF model IFS ensemble forecast system. ~~Three experiments were conducted,~~ In addition to the operational ensemble forecast ~~with the perturbation at initial conditions,~~ the TOT ensemble, some other experiments have been carried out, the initial condition perturbation ensemble,
915 INI, ~~two experiments and two ensembles~~ with SPP, in one case perturbing only the parameters of the convection parameterization, SPP-Conv, and in the other perturbing the parameters of all relevant physical parameterizations, SPP. The ~~used approach has been aimed at the analysis first and foremost of tracking and intensity, meaning central pressure. Secondly, the precipitation field has been analyzed, and finally, the focus has been put on the~~ approach used was aimed at analyzing the
920 ~~tracks, intensity, i.e. central pressure, precipitation, and~~ parameters characterizing the thermal structure of the ~~cyclone and its asymmetry, the convective heating and the development processes~~ cyclones. Secondly, the processes behind the generation and development of the cyclones have been analyzed in conjunction with the previous analysis.

~~From the study, it was found that the~~ The result of this study, compared to previous ones (Di Muzio et al., 2019; Chaboureau et al., 2012;
, which used only the operation ensemble forecast of ECMWF, points out the benefit of using the Stochastically Perturbed
925 Parameterization, SPP ensemble forecast compared to just perturbing the initial conditions. The use of SPP, and specifically in particular the perturbation of convective parameters (SPP-Conv), was found to compare well with the INI and TOT experiments
in terms of tracking ~~spread and precipitation intensity compare well to the INI experiment,~~ cyclone intensity and precipitation.
Similar results have been obtained ~~also~~ in Ollinaho et al. (2017), especially regarding precipitation. The ~~three~~ experiments are usually ~~under dispersive when it comes to~~ underdispersive in terms of tracking position, ~~even if the INI experiment is giving~~
930 ~~although the TOT experiment gives~~ better results. ~~It has to be noted that the~~ Indeed, the ensemble forecast TOT has proven to be the best in terms of spread and error compared to the tracking, intensity and precipitation of cyclones. This is due to the inclusion of the model's physics perturbation, in line with what was found in Lang et al. (2021). The ensemble spread and mean are usually generally lower in the SPP experiments. Nonetheless the latter For instance, the analysis of the thermal structure and symmetry shows that for the upper-level thermal wind, the smaller spread is obtained in most cases in the SPP-Conv experiment
935 (in particular at later forecasts). Nonetheless, the two SPP ensembles are able to produce the same spread as the initial condition perturbation experiment , underlying at later time steps, highlighting the benefit of the introduction of perturbations of physical parameters , especially regarding convection, in comparison with only using the introducing physical parameters perturbations, especially with respect to convection, compared to use only perturbations of the initial conditions (Lang et al., 2012; Ollinaho et al., 2017). Moreover, the similarity of the SPP and the SPP-Conv results, especially for the thermal structure and thermal
940 asymmetry, highlights that the uncertainties linked to the convection parameterization are predominant in the simulation of these types of phenomena, confirming previous results (Pytharoulis, 2018; Fink et al., 2012; Wimmer et al., 2022). Finally, with respect to the above-mentioned cyclone characteristics, it is found that there is a common gradual decrease in the error with the forecast starting date closer to the occurrence. This is consistent for all three ensemble experiments and it is specific for Ianos and Zorbas. For Trixie this decrease in the error is weaker and, in some cases, non-existent. Indeed, as pointed out in
945 the results the simulation of this particular cyclone can be considered as a missed forecast (as shown by the track in Fig. 1 and

the intensity in Fig. 4).

Regarding ~~Specifically, regarding~~ the reproduction of the minimum central pressure by the ensemble forecasts (~~Figure 4~~) ~~it is found that in general there is~~ Fig. 4) ~~there is generally~~ a time shift in the reproduction of the minimum intensity, where
950 both the Ianos and Zorbas ensemble ~~mean means~~ reach the maximum intensity with a delay. Since the delay ~~is decreasing with~~
~~forecast start date closer to occurrence~~ ~~decreases as the forecast starting date gets closer to the event~~, this is ~~attributable to due~~
~~to the~~ improved initial conditions. ~~Regarding Ianos and Zorbas,~~ ~~Indeed,~~ ~~it is found that the maximum intensity is reached when~~
~~the upper-level PV streamer and the ensemble spread for surface-level vortex are aligned, and the latter is better captured by~~
~~starting the simulation closer to the cyclone's onset. This is consistent with what was found in Flaounas et al. (2015) where~~
955 ~~they underlined that the intensity of the surface cyclone increases while the streamer is on the western side of the cyclone and~~
~~begins to decrease as the streamer is wrapping over its centre. It is noteworthy that for Zorbas the intense phase (i.e. low values~~
~~of minimum core pressure) is maintained for a longer period, compared to the SPP experiments is able to include the analysis~~
~~one, similarly to the INI experiment (Figure 4) operational analysis, as underlined by the minimum core pressure trend in Fig.~~
~~4, and by the PV tower reported in Fig. 12. This is probably due to the fact that most members (especially regarding the SPP~~
960 ~~ensembles) spend most of their lives at sea and do not cross land over Greece, thus managing to sustain themselves for a longer~~
~~period through condensational heating and air-sea interaction.~~

~~By Then, by~~ looking at the simulated precipitation distribution, compared to the GPM-IMERG satellite observations, ~~show~~
~~it is shown~~ that only for Ianos, the precipitation field is well reproduced by the ensembles, with the ~~INI-SPP~~ experiment being
965 slightly more intense than the ~~SPP and SPP-Conv experiments others~~. Even if the GPM-IMERG dataset ~~tends to overes-~~
~~timate the precipitation over the Mediterranean , the precipitation simulated (Peinó et al., 2022; Caracciolo et al., 2018), the~~
~~simulated precipitation~~ for Zorbas and Trixie is too weak. However, it is discussed that in general, the precipitation maximum
compares better with ~~forecast start the forecasts starting~~ date closer to ~~the~~ occurrence, thus for Zorbas, starting the ensemble
forecasts on the 28th would have shown better-simulated precipitation. ~~However, the precipitation maximum values are~~
970 ~~slightly better simulated by the INI experiment also for Zorbas. The analysis of the precipitation field deepened by computing~~
~~some statistical scores and the results show that the SPP-Conv is slightly better than the SPP and INI experiment. The BS~~
~~score results are quite similar between the three experiments and generally show how the three ensemble forecasts perform~~
~~better than the control forecast. Furthermore, all three forecasts present useful values in terms of precipitation prediction~~
~~(Buizza et al., 2008), being higher than 0.5 and in most cases higher than 0.7. The most significant values, occur in Ianos,~~
975 ~~making it the most well-captured storm of the three. It could be argued that a finer resolution than a 9 km resolution would~~
~~improve the reproduction of the intensity and track of the tropical-like Mediterranean cyclones. A recent single forecast~~
~~experimental tropical cyclone simulations at 4 km resolution by (Majumdar et al., 2023) reveal that the 4 km simulations~~
~~produce deeper and more realistic tropical cyclones in terms of radial wind structure compared to the observations than~~
~~the 9 km forecasts. However, in the aforementioned work done within the DestinE project (Gascón et al., 2023), preliminary~~
980 ~~simulations carried out with IFS at 4 km resolution did not show any significant changes in the simulated tracks and intensity~~

of Medicanes, except for slightly more intense winds. This applies to both Trixie (<https://confluence.ecmwf.int/x/soQvEQ>) and Ianos (<https://confluence.ecmwf.int/x/soQvEQ>) where the 9 and 4 km resolution simulations are roughly equivalent.

985 ~~Regarding the tracking,~~ It is shown that for Ianos and Zorbas the forecasts are accurate at reproducing both the thermal structure and symmetry of the cyclones, compared to the analysis value. The only exception to the reasonable reproduction of the storm thermal structure is the upper-level thermal wind in Trixie (Fig. 6a-c-e). This means that for Trixie, where the analysis value reported the presence of a warm core ($-V_T^U = 25$ in Table 2), the ~~precipitation and the intensity of the cyclone~~ there is a common gradual decrease of the error with forecast start date closer to occurrence. This is consistent for all three ensemble experiments and it ~~three ensemble forecast presents a cold core cyclone (negative $-V_T^U$ values).~~ This, together with 990 ~~the underestimation of the deepening of the cyclone,~~ can explain the simulated precipitation being weaker than the observations since the simulated cyclone is specific for Ianos and Zorbas. Usually, the later starting forecasts tend to be more accurate (lower error and spread). For Trixie this decrease in the error is weaker and in some cases nonexistent. Indeed, as pointed out in the results the simulation of this particular cyclone can be considered a missed forecast ~~not able to reach the warm core,~~ thus the convective heating is lower affecting the simulation of the precipitation. From the Q1 and Q2 profiles, it is evinced that the 995 ~~cyclone seems to intensify around the 28th and to die out by the 30th, when it should have entered the tropical phase, as mentioned in Dafis et al. (2020).~~

~~Through~~ ~~Indeed,~~ ~~through~~ tracking, it was verified that with regard to the Trixie simulation, there is a southeastward shift of the trajectory with respect to the analysis ~~and, that, among the three storms, the best predicted is Ianos. The southeastward shift was identified after the analysis of the ensemble spread and error~~(Fig. 1). A lower spread in the tracked position was found for Zorbas and Ianos compared to Trixie, but the error of Trixie exceeds 800 km. This is attributable to the fact that the ensemble forecast starts too early with respect to the cyclone intensification phase for Trixie. This result, in particular, aligns with previous studies that had pointed to Trixie's low occurrence probability up to two days earlier (Di Muzio et al., 2019). Indeed, There is an inherently low probability of medicanes occurrence (as seen in Di Muzio et al. (2019)) and the development of a warm 1000 core cyclone depends on many factors, large-scale factors and ~~small-scale factors like~~ surface fluxes, that can be improved by the initial conditions of a preexisting cyclone. ~~The decrease of the spread at later starting dates in Trixie can be correlated with the higher probability of occurrence and the better reproduction of the physical processes leading to cyclone intensification.~~

~~Indeed, the factors that have played a role in the forecasts missing the tracking~~ In order to evaluate the obtained results, 1010 ~~an investigation of the development processes and their simulation were linked to the forecasts track~~ position and intensification ~~have been found to be linked to the simulations of the development processes. Besides the missing intensification of the precursor of each cyclone. First, it has been pointed out that Ianos, Zorbas, and Trixie all require the presence of a PV streamer together with a deep cut-off low, the factor that has been recognized to be of primary importance in low in order to form. This underlines the nature of these cyclones as being born in a baroclinically unstable environment. This is initially reproduced reasonably well, although specifically in the case of Trixie, the ensembles may have started too early to capture~~

the interaction between the two, making Trixie a weaker cyclone and ultimately leading to its ending. As pointed out in the previous section, the development of these types of Mediterranean cyclones is the simulation of the alignment between the upper-level and the lower-level regions with high values of PV (Carrió et al., 2017; Cioni et al., 2018; Flaounas et al., 2022). This happens specifically for Trixie, but it is also true for Ianos and Zorbas, especially with the timing shift with which they intensify. cut-off low which contributes to the development of Trixie quickly weakens in the ensemble simulations after the 29th and is then shut down in favour of another one that crossed the Ionian sea (Supplementary Fig. S4 and S5).

By the analysis of the cyclone thermal structure and symmetry and the Q1 and Q2 profiles, it is shown that if for Ianos and Zorbas the tropical-like phase is reached, with a gradual evolution of the error and spread, where there is a lowering of the spread accompanied by the distribution approaching the reference values (upper-level thermal wind in Figure ?? and ??). In those cases, it has been shown that after the formation of the three cyclones, the operational analysis represents a clear interaction between the surface level vortex and the PV anomaly in the upper troposphere in all three cases, the forecasts are accurate at reproducing both the thermal structure and symmetry of the cyclones, compared to the analysis value. Both Zorbas and Ianos deep warm core phase is well captured, especially with forecast start date closer to occurrence.

The only exception to the reasonable reproduction of the storm thermal structure is the upper-level thermal wind in Trixie (Figures ??a-e). This means that for Trixie, where the analysis value reported the presence of a warm core ($-V_T^U = 25$ in Table 2), the three ensemble forecast presents a cold core cyclone (negative $-V_T^U$ values). This, together with the underestimation of the deepening of the cyclone, can explain the low scores for the precipitation analysis since the simulated cyclone is not able to reach the warm core, thus the convective heating is lower affecting the simulation of the precipitation. From the Q1 and Q2 profiles, it is evinced that the cyclone seems to intensify around the 28th and to die out by the 30th, when it was actually supposed to enter the PV tower, in order for them to intensify and eventually reach “tropical-like phase. Also in Dafis et al. (2020) it was reported that a second intensification occurred in Trixie around the 30th due to deep convection activity.

In general, the analysis of features (Carrió et al., 2017; Cioni et al., 2018; Flaounas et al., 2022). This is present in the ensembles (both for SPP and INI) in the case of Ianos and Zorbas, where, the thermal structure and symmetry indicates that for the upper-level thermal wind, PV anomaly brought by the PV streamer is able to match with the lower-level PV production by diabatic processes. As also pointed out, this surface cyclone is sustained by convective heating release by condensation, with surface fluxes supporting the cyclone in the smaller spread is in most cases obtained in the SPP-Conv experiment (in particular at later forecasts), while most intense phase along with convective activity (Supplementary Fig. S7). In the spread is comparable for the three ensemble experiments regarding the thermal symmetry. This once again points out the possibility of using SPP in ensemble forecasting to generate a similar spread in the ensemble distributions compared to only using initial conditions perturbations. Indeed the ensemble experiments behave similarly regarding the simulation of the tropical-like characteristics of the three cyclones. Furthermore, the SPP and SPP-Conv experiments are found to be extremely similar, possibly meaning that the uncertainties linked to the convection parameterization are predominant in the simulation of these types of phenomena.

1050 To answer the question of why Trixie has not been well simulated in comparison with the other two medicanes presented in
the study, the analysis of the synoptic situation and physical process involved in the genesis and maintenance of the medicanes
has been carried out. From the analysis of the 2 PV isosurfaces and the PV field cross-section revealed that the interaction
between the upper-level stratospheric PV intruding in the upper troposphere and the lower-level PV generated by convective
1055 heating is key for the intensification and maintenance of Trixie. The later the starting date the greater the misalignment (or case
of Ianos, the convective activity peaks during the moist intense phase, as underlined by the PV anomaly in the worse positioning
of PV cross-section in Fig. 11, while in the case of Zorbas, convective activity is present also before the cyclone tropical like
phase (as also underlined by the PV anomaly in Fig. 11). The ensemble simulated cyclones are sensitive to the upper-level
disturbance) between the lower and the upper PV production. As mentioned earlier, this is in line with what was found in
the literature. Indeed, in many positioning of the PV streamer, which, as observed in the literature, has a clear impact on the
1060 simulation of the medicane. In the case of Zorbas, as noted in Portmann et al. (2020), a westward shift of the PV streamer leads
on average to weaker cyclones, which can be observed in the ensemble mean of Zorbas in Fig. 4. The displacement of the PV
streamer is linked to the alignment with the surface level and the consequent creation of a PV tower. Furthermore, the intensity
of the PV anomalies, as well as the height reached by the 2 PVU isosurface, may have played a role in the cyclone's greater or
lesser intensity. In fact, in the case of Ianos, it can be argued that the cyclone is more intense in the ensembles compared to the
1065 analysis due to the higher simulated PV anomaly and deeper PV streamer. In other studies, also using the ECMWF ensemble
forecasting system (Portmann et al., 2020; Chaboureau et al., 2012)(Chaboureau et al., 2012), it was found that later forecasts
are able to capture better the thermal structure of the medicanes, due to the lower uncertainty of the positioning of PV streamer
connected to the generation of the medicane. In general, in our study is assessed that the earlier the starting date the greater the
misalignment (or the worse positioning of the upper-level disturbance) between the lower and the upper PV production. This
1070 is true not only, particularly in the case of Trixie but also in Zorbas and Ianos, where the error and the spread are lowered for
the ensemble forecasts due to the better reproduction of these features, where on the simulation starting too early, on the 25th,
the lower level PV production is absent, and for the simulation starting on the 26th and the 27th it is very weak and not able to
be reinforced by the upper level one.

1075 However, in the case of Trixie, it also has to be noticed that the fact that it is Trixie is also a weaker medicane compared
to Ianos and Zorbas influences the simulations. Indeed, (the central minimum pressure of Trixie is lower than the other two
cyclones, as reported in Table 2), influencing the simulations. In a recent study by (Panegrossi et al., 2023), while Ianos and
Zorbas have been recognized as two of the most intense medicanes, Trixie has been characterized as one of the weakest,
not even reaching the status of deep warm core, as established by looking at passive microwave measurements and products.
1080 Here, it has been shown firstly that the surface fluxes in the phase of tropicalization and intensification are lower than the
other medicanes and the eyelone. Secondly, it is underlined that the SST anomaly in the case of Trixie was low both in the
analysis and in the ensembles, yielding to a weaker cyclone, and lastly that Trixie tends to shut off when the cut-off low
vanishes and generally tend in the simulations and generally tends to follow the PV streamer position. This makes it more
subject to being more dependent on the simulation of large-scale processes and more prone to being simulated more weakly

1085 than the other two. The three medicanes seem to belong to different medicanes categories of the medicanes classification (Miglietta and Rotunno, 2019; Dafis et al., 2020; Flaounas et al., 2022). Specifically, in Miglietta and Rotunno (2019) and Flaounas et al. (2022) three distinct categories of medicanes are distinguished: one in which baroclinic instability plays an important role throughout the cyclone's lifetime and most of their intensification is due to convection (Fita and Flaounas, 2018); and, More specifically the lower level PV production present in the analysis in Fig. 11 is absent in the simulations in Fig. 12. Since the surface fluxes and the anomaly of SST do not play a role, this makes the convective instability brought by the cutoff low necessary to sustain the cyclone convection. The deep cut-off low absence in the simulations can be linked to the medicanes missing development in the case of Trixie. This is supported by the findings of Fischer et al. (2017), who hypothesized that tropical cyclones intensification rate after tropical cyclogenesis, in environments of upper-tropospheric troughs, is closely linked to the structure and temporal evolution of the upper-level trough.

1095 Going back to the medicanes classification, the three medicanes seem to belong to different medicanes categories. Ianos and Zorbas seem to belong to the one in which baroclinicity is important only in the initial stage and, the theory of wind-induced surface heat exchange (WISHE (Emanuel, 1986)) is behind their intensification through positive feedback between the latent heat release and the air-sea interactions and is behind their intensification through Flaounas et al. (2022). Trixie seems to belong to the one in which there is a synergy between baroclinic and diabatic processes (and control from the SST over the cyclone (Pytharoulis et al., 2000)). The first type is possibly Trixie's family and Ianos and Zorbas belong to the second and third types respectively. Thus in baroclinic instability plays an important role throughout the cyclone's lifetime and most of their intensification is due to convection (Fita and Flaounas, 2018). Thus, one of the outcomes of this study, it is found is that the ensemble forecasting of ECMWF is likely able to better capture the tropical-like features of the second and third categories of first category of medicanes. The investigation of this will be the subject of further study, also considering a greater number of medicanes. This analysis also underlines the different sensitivity of the diabatic processes in the simulation of these medicanes, because it makes it clear that convective heating has played a major role in the intensification of the cyclones and when absent is linked to the disappearance of the cyclone itself, as in the case of Trixie.

1105 To sum up, by considering all the parameters used in this analysis, it can be assessed that the ECMWF ensemble forecasts model can adequately reproduce medicanes with their tropical-like features, given a correct representation of the large-scale circulation. The result of this study, compared to previous ones (Di Muzio et al., 2019; Chaboureaud et al., 2012; Pantillon et al., 2013) which used only the operation ensemble forecast of ECMWF, points out the benefit of using the Stochastically Perturbed Parameterization, SPP ensemble forecast compared to only perturbing the initial conditions. The SPP, especially the SPP-Conv experiments, show in some cases lower but comparable spread and spread-skill score values and better precipitation scores than the INI experiment.

1115 Regarding the physical processes linked to the ensemble forecasting results To conclude, this study confirms that similar processes are at play in the development of the Mediterranean tropical-like cyclones and the predictability of these cyclones is linked to not only the reproduction of the precursor events (namely the deep cut-off low) but also to the interaction of the upper-level dynamics with the lower-level one (namely the PV streamer and the lower level PV production), in a similar way.

1120 This work, as urged in the literature (Dafis et al., 2020; Pytharoulis, 2018) underlines the relative importance of the upper-tropospheric troughs and PV streamer interactions with the troposphere for medicanes not only in one specific case, as often done in the literature (Portmann et al., 2020; Chaboureau et al., 2012; Cioni et al., 2018), but extending the analysis at least to a few different cases.

1125 Finally, as discussed in Flaounas et al. (2022) the representation of cloud adiabatic processes is often believed to be a source of forecast uncertainty but dominated by the one created by initial conditions. This study, by comparing ensemble forecasts with the account of initial condition perturbation only and of physical parameterization only, underlines that the uncertainty produced by both ensembles is actually similar. ~~This is due to the found similar spread/skill relationship for the tracking and similar scores for what concerns the intensity of precipitation and the reproduction of the cyclone intensity.~~

1130 *Code and data availability.* The output of the IFS ensemble forecasts and the operational analysis data are available on the MARS Archive at <https://www.ecmwf.int/en/forecasts/dataset/ecmwf-research-experiments> and the precipitation dataset GPM-IMERG used for validation is freely available on the NASA data archives at <https://gpm.nasa.gov/data/imerg>. The python codes used to produce the analysis are available at <https://doi.org/10.5281/zenodo.7912957>.

Author contributions. All authors contributed to the conceptualization of the research. P.B., M.S., and P.B.C. worked on the methodology. 1135 P.B. carried out the ensemble simulations. M.S. and L.S. carried out the analysis of the ensemble simulations and P.B.C. supervised all the research group work. M.S. and P.B. wrote the original draft. All authors have read, reviewed, edited, and agreed to the manuscript.

Competing interests. No competing interests are present

Acknowledgements. This research has been funded by the Italian Ministry of University and Research (MIUR) and the University of Perugia within the program *Dipartimenti di Eccellenza 2018-2022*, by the ~~Fondo Ricerca di Ateneo esercizio 2021: Cambiamenti climatici: eonsapevolezza impatto sociale, modelli scientifici e soluzioni tecnologiche~~ and by the European Centre of Medium Range Weather Forecast (ECMWF), ~~by the Fondo Ricerca di Ateneo esercizio 2021: Cambiamenti climatici: eonsapevolezza impatto sociale, modelli scientifici e soluzioni tecnologiche~~ and by the CIRIAF (Centro Interuniversitario di Ricerca sull'Inquinamento e sull'Ambiente "Mauro Felli") - SSTAM with the research project Modelli predittivi ad alta definizione per fenomeni meteo-climatici nell'ambiente mediterraneo. This article is a contribution to the COST Action CA19109 "MedCyclones: European Network for Mediterranean Cyclones in weather and climate"; The 1145 authors are grateful to Simon Lang and Martin Leutbecher for developing and providing the experimental SPP configuration and want to acknowledge high-performance computing support from ECMWF Supercomputing HPC facilities.

References

- Baker, L., Rudd, A., Migliorini, S., and Bannister, R.: Representation of model error in a convective-scale ensemble prediction system, *Nonlinear Processes in Geophysics*, 21, 19–39, 2014.
- 1150 Bechtold, P., Köhler, M., Jung, T., Doblas-Reyes, F., Leutbecher, M., Rodwell, M. J., Vitart, F., and Balsamo, G.: Advances in simulating atmospheric variability with the ECMWF model: From synoptic to decadal time-scales, *Quarterly Journal of the Royal Meteorological Society: A journal of the atmospheric sciences, applied meteorology and physical oceanography*, 134, 1337–1351, 2008.
- Beljaars, A. C., Brown, A. R., and Wood, N.: A new parametrization of turbulent orographic form drag, *Quarterly Journal of the Royal Meteorological Society*, 130, 1327–1347, 2004.
- 1155 Brier, G. W. et al.: Verification of forecasts expressed in terms of probability, *Monthly weather review*, 78, 1–3, 1950.
- Buizza, R.: The value of probabilistic prediction, *Atmospheric Science Letters*, 9, 36–42, 2008.
- Buizza, R. and Hollingsworth, A.: Storm prediction over Europe using the ECMWF ensemble prediction system, *Meteorological Applications*, 9, 289–305, 2002.
- Buizza, R., Milleer, M., and Palmer, T. N.: Stochastic representation of model uncertainties in the ECMWF ensemble prediction system, *Quarterly Journal of the Royal Meteorological Society*, 125, 2887–2908, 1999.
- 1160 Buizza, R., Leutbecher, M., and Isaksen, L.: Potential use of an ensemble of analyses in the ECMWF Ensemble Prediction System, *Quarterly Journal of the Royal Meteorological Society: A journal of the atmospheric sciences, applied meteorology and physical oceanography*, 134, 2051–2066, 2008.
- Caracciolo, D., Francipane, A., Viola, F., Noto, L. V., and Deidda, R.: Performances of GPM satellite precipitation over the two major
1165 Mediterranean islands, *Atmospheric Research*, 213, 309–322, 2018.
- Carrió, D., Homar, V., Jansa, A., Romero, R., and Picornell, M.: Tropicalization process of the 7 November 2014 Mediterranean cyclone: Numerical sensitivity study, *Atmospheric Research*, 197, 300–312, 2017.
- Carrió, D., Homar, V., Jansà, A., Picornell, M., and Campins, J.: Diagnosis of a high-impact secondary cyclone during HyMeX-SOP1 IOP18, *Atmospheric Research*, 242, 104 983, 2020.
- 1170 Cavicchia, L., von Storch, H., and Gualdi, S.: A long-term climatology of medicanes, *Climate dynamics*, 43, 1183–1195, 2014.
- Chaboureaud, J. P., Pantillon, F., Lambert, D., Richard, E., and Claud, C.: Tropical transition of a Mediterranean storm by jet crossing, *Quarterly Journal of the Royal Meteorological Society*, 138, 596–611, <https://doi.org/10.1002/qj.960>, 2012.
- Christensen, H. M., Moroz, I., and Palmer, T.: Stochastic and perturbed parameter representations of model uncertainty in convection parameterization, *Journal of the Atmospheric Sciences*, 72, 2525–2544, 2015.
- 1175 Cioni, G., Malguzzi, P., and Buzzi, A.: Thermal structure and dynamical precursor of a Mediterranean tropical-like cyclone, *Quarterly Journal of the Royal Meteorological Society*, 142, 1757–1766, 2016.
- Cioni, G., Cerrai, D., and Klocke, D.: Investigating the predictability of a Mediterranean tropical-like cyclone using a storm-resolving model, *Quarterly Journal of the Royal Meteorological Society*, 144, 1598–1610, 2018.
- Claud, C., Alhammoud, B., Funatsu, B. M., and Chaboureaud, J.-P.: Mediterranean hurricanes: large-scale environment and convective and
1180 precipitating areas from satellite microwave observations, *Natural Hazards and Earth System Sciences*, 10, 2199–2213, 2010.
- Comellas Prat, A., Federico, S., Torcasio, R. C., D’Adderio, L. P., Dietrich, S., and Panegrossi, G.: Evaluation of the Sensitivity of Mediane Ianos to Model Microphysics and Initial Conditions Using Satellite Measurements, *Remote Sensing*, 13, 4984, 2021.

- Dafis, S., Claud, C., Kotroni, V., Lagouvardos, K., and Rysman, J.-F.: Insights into the convective evolution of Mediterranean tropical-like cyclones, *Quarterly Journal of the Royal Meteorological Society*, 146, 4147–4169, 2020.
- 1185 Davis, C.: Resolving tropical cyclone intensity in models, *Geophysical Research Letters*, 45, 2082–2087, 2018.
- Davolio, S., Miglietta, M., Moscatello, A., Pacifico, F., Buzzi, A., and Rotunno, R.: Numerical forecast and analysis of a tropical-like cyclone in the Ionian Sea, *Natural Hazards and Earth System Sciences*, 9, 551–562, 2009.
- Di Muzio, E., Riemer, M., Fink, A. H., and Maier-Gerber, M.: Assessing the predictability of Medicanes in ECMWF ensemble forecasts using an object-based approach, *Quarterly Journal of the Royal Meteorological Society*, 145, 1202–1217, 2019.
- 1190 Donlon, C. J., Martin, M., Stark, J., Roberts-Jones, J., Fiedler, E., and Wimmer, W.: The operational sea surface temperature and sea ice analysis (OSTIA) system, *Remote Sensing of Environment*, 116, 140–158, 2012.
- Emanuel, K.: Genesis and maintenance of "Mediterranean hurricanes", *Advances in Geosciences*, 2, 217–220, 2005.
- Emanuel, K. A.: An air-sea interaction theory for tropical cyclones. Part I: Steady-state maintenance, *Journal of Atmospheric Sciences*, 43, 585–605, 1986.
- 1195 Ernst, J. and Matson, M.: A Mediterranean tropical storm?, *Weather*, 38, 332–337, 1983.
- Fink, A. H., Pohle, S., Pinto, J. G., and Knippertz, P.: Diagnosing the influence of diabatic processes on the explosive deepening of extratropical cyclones, *Geophysical Research Letters*, 39, 2012.
- Fischer, M. S., Tang, B. H., and Corbosiero, K. L.: Assessing the influence of upper-tropospheric troughs on tropical cyclone intensification rates after genesis, *Monthly Weather Review*, 145, 1295–1313, 2017.
- 1200 Fita, L. and Flaounas, E.: Medicanes as subtropical cyclones: The December 2005 case from the perspective of surface pressure tendency diagnostics and atmospheric water budget, *Quarterly Journal of the Royal Meteorological Society*, 144, 1028–1044, 2018.
- Flaounas, E., Raveh-Rubin, S., Wernli, H., Drobinski, P., and Bastin, S.: The dynamical structure of intense Mediterranean cyclones, *Climate Dynamics*, 44, 2411–2427, 2015.
- Flaounas, E., Kotroni, V., Lagouvardos, K., Gray, S. L., Rysman, J.-F., and Claud, C.: Heavy rainfall in Mediterranean cyclones. Part I: contribution of deep convection and warm conveyor belt, *Climate dynamics*, 50, 2935–2949, 2018.
- 1205 Flaounas, E., Gray, S. L., and Teubler, F.: A process-based anatomy of Mediterranean cyclones: from baroclinic lows to tropical-like systems, *Weather and Climate Dynamics*, 2, 255–279, 2021.
- Flaounas, E., Davolio, S., Raveh-Rubin, S., Pantillon, F., Miglietta, M. M., Gaertner, M. A., Hatzaki, M., Homar, V., Khodayar, S., Korres, G., et al.: Mediterranean cyclones: Current knowledge and open questions on dynamics, prediction, climatology and impacts, *Weather and Climate Dynamics*, 3, 173–208, 2022.
- 1210 Forbes, R. M., Tompkins, A. M., and Untch, A.: A new prognostic bulk microphysics scheme for the IFS, 2011.
- Frogner, I.-L., Andrae, U., Ollinaho, P., Hally, A., Hämäläinen, K., Kauhanen, J., Ivarsson, K.-I., and Yazgi, D.: Model uncertainty representation in a convection-permitting ensemble—SPP and SPPT in HarmonEPS, *Monthly Weather Review*, 150, 775–795, 2022.
- Gascón, E., Sandu, I., Vannièrè, B., Magnusson, L., Forbes, R., Polichtchouk, I., Van Niekerk, A., Sützl, B., Maier-Gerber, M., Diamantakis, M., et al.: Advances towards a better prediction of weather extremes in the Destination Earth initiative, Tech. rep., Copernicus Meetings, 2023.
- 1215 Geetha, B. and Balachandran, S.: Diabatic heating and convective asymmetries during rapid intensity changes of tropical cyclones over North Indian Ocean, *Tropical Cyclone Research and Review*, 5, 32–46, 2016.
- Goosse, H. and Fichefet, T.: Importance of ice-ocean interactions for the global ocean circulation: A model study, *Journal of Geophysical Research: Oceans*, 104, 23 337–23 355, 1999.
- 1220

- Grabowski, W. W., Wu, X., and Moncrieff, M. W.: Cloud resolving modeling of tropical cloud systems during Phase III of GATE. Part III: Effects of cloud microphysics, *Journal of the atmospheric sciences*, 56, 2384–2402, 1999.
- Hamill, T. M., Whitaker, J. S., Fiorino, M., and Benjamin, S. G.: Global ensemble predictions of 2009’s tropical cyclones initialized with an ensemble Kalman filter, *Monthly Weather Review*, 139, 668–688, 2011.
- 1225 Hart, R. E.: A cyclone phase space derived from thermal wind and thermal asymmetry, *Monthly weather review*, 131, 585–616, 2003.
- Hart, R. E. and Evans, J. L.: A climatology of the extratropical transition of Atlantic tropical cyclones, *Journal of Climate*, 14, 546–564, 2001.
- Hogan, R. J. and Bozzo, A.: A flexible and efficient radiation scheme for the ECMWF model, *Journal of Advances in Modeling Earth Systems*, 10, 1990–2008, 2018.
- 1230 Homar, V., Romero, R., Stensrud, D., Ramis, C., and Alonso, S.: Numerical diagnosis of a small, quasi-tropical cyclone over the western Mediterranean: Dynamical vs. boundary factors, *Quarterly Journal of the Royal Meteorological Society: A journal of the atmospheric sciences, applied meteorology and physical oceanography*, 129, 1469–1490, 2003.
- Huffman, G. J., Bolvin, D. T., Braithwaite, D., Hsu, K.-L., Joyce, R. J., Kidd, C., Nelkin, E. J., Sorooshian, S., Stocker, E. F., Tan, J., et al.: Integrated multi-satellite retrievals for the global precipitation measurement (GPM) mission (IMERG), in: *Satellite precipitation measurement*, pp. 343–353, Springer, 2020.
- 1235 IFS Documentation CY47R3, E.: IFS Documentation CY47R3 Part IV Physical processes, 2021a.
- IFS Documentation CY47R3, E.: IFS Documentation CY47R3 Part V Ensemble prediction system, 2021b.
- IFS Documentation CY47R3, E.: IFS Documentation CY47R3 Part VII ECMWF Wave model, 2021c.
- Köhler, M., Ahlgrim, M., and Beljaars, A.: Unified treatment of dry convective and stratocumulus-topped boundary layers in the ECMWF
- 1240 model, *Quarterly Journal of the Royal Meteorological Society*, 137, 43–57, 2011.
- Koseki, S., Mooney, P. A., Cabos, W., Gaertner, M. Á., de la Vara, A., and González-Alemán, J. J.: Modelling a tropical-like cyclone in the Mediterranean Sea under present and warmer climate, *Natural Hazards and Earth System Sciences*, 21, 53–71, 2021.
- Lagouvardos, K., Karagiannidis, A., Dafis, S., Kalimeris, A., and Kotroni, V.: Ianos—A hurricane in the Mediterranean, *Bulletin of the American Meteorological Society*, 103, E1621–E1636, 2022.
- 1245 Lang, S., Leutbecher, M., and Jones, S.: Impact of perturbation methods in the ECMWF ensemble prediction system on tropical cyclone forecasts, *Quarterly Journal of the Royal Meteorological Society*, 138, 2030–2046, 2012.
- Lang, S. T., Lock, S.-J., Leutbecher, M., Bechtold, P., and Forbes, R. M.: Revision of the stochastically perturbed parametrisations model uncertainty scheme in the integrated forecasting system, *Quarterly Journal of the Royal Meteorological Society*, 147, 1364–1381, 2021.
- Leutbecher, M., Lock, S.-J., Ollinaho, P., Lang, S. T., Balsamo, G., Bechtold, P., Bonavita, M., Christensen, H. M., Diamantakis, M., Dutra,
- 1250 E., et al.: Stochastic representations of model uncertainties at ECMWF: State of the art and future vision, *Quarterly Journal of the Royal Meteorological Society*, 143, 2315–2339, 2017.
- Lin, J. and Qian, T.: Rapid intensification of tropical cyclones observed by AMSU satellites, *Geophysical Research Letters*, 46, 7054–7062, 2019.
- Magnusson, L., Thorpe, A., Buizza, R., Rabier, F., and Nicolau, J.: Predicting this year’s European heat wave, *ECMWF Newsletter*, 145, 4–5, 2015.
- 1255 Majumdar, S. J. and Torn, R. D.: Probabilistic verification of global and mesoscale ensemble forecasts of tropical cyclogenesis, *Weather and Forecasting*, 29, 1181–1198, 2014.

- Majumdar, S. J., Magnusson, L., Bechtold, P., Bidlot, J.-R., and Doyle, J. D.: Advanced tropical cyclone prediction using the experimental global ECMWF and operational regional COAMPS-TC systems, *Monthly weather review*, 2023.
- 1260 Malardel, S., Wedi, N., Deconinck, W., Diamantakis, M., Kühnlein, C., Mozdzyński, G., Hamrud, M., and Smolarkiewicz, P.: A new grid for the IFS, *ECMWF newsletter*, 146, 321, 2016.
- Marsigli, C., Montani, A., and Paccagnella, T.: A spatial verification method applied to the evaluation of high-resolution ensemble forecasts, *Meteorological Applications: A journal of forecasting, practical applications, training techniques and modelling*, 15, 125–143, 2008.
- Mazza, E., Ulbrich, U., and Klein, R.: The tropical transition of the October 1996 medicane in the western Mediterranean Sea: A warm
1265 seclusion event, *Monthly Weather Review*, 145, 2575–2595, 2017.
- McTaggart-Cowan, R., Davies, E. L., Fairman, J. G., Galarneau, T. J., and Schultz, D. M.: Revisiting the 26.5° C sea surface temperature threshold for tropical cyclone development, *Bulletin of the American Meteorological Society*, 96, 1929–1943, 2015.
- Miglietta, M., Laviola, S., Malvaldi, A., Conte, D., Levizzani, V., and Price, C.: Analysis of tropical-like cyclones over the Mediterranean Sea through a combined modeling and satellite approach, *Geophysical Research Letters*, 40, 2400–2405, 2013.
- 1270 Miglietta, M., Cerrai, D., Laviola, S., Cattani, E., and Levizzani, V.: Potential vorticity patterns in Mediterranean “hurricanes”, *Geophysical Research Letters*, 44, 2537–2545, 2017.
- Miglietta, M. M. and Rotunno, R.: Development mechanisms for Mediterranean tropical-like cyclones (medicanes), *Quarterly Journal of the Royal Meteorological Society*, 145, 1444–1460, 2019.
- Miglietta, M. M., Moscatello, A., Conte, D., Mannarini, G., Lacorata, G., and Rotunno, R.: Numerical analysis of a Mediterranean ‘hurricane’ over south-eastern Italy: Sensitivity experiments to sea surface temperature, *Atmospheric research*, 101, 412–426, 2011.
- 1275 Miglietta, M. M., Mastrangelo, D., and Conte, D.: Influence of physics parameterization schemes on the simulation of a tropical-like cyclone in the Mediterranean Sea, *Atmospheric Research*, 153, 360–375, 2015.
- Mogensen, K., Keeley, S., and Towers, P.: Coupling of the NEMO and IFS models in a single executable, *ECMWF Reading, United Kingdom*, 2012.
- 1280 Montani, A., Cesari, D., Marsigli, C., and Paccagnella, T.: Seven years of activity in the field of mesoscale ensemble forecasting by the COSMO-LEPS system: main achievements and open challenges, *Tellus A: Dynamic Meteorology and Oceanography*, 63, 605–624, 2011.
- Moscatello, A., Marcello Miglietta, M., and Rotunno, R.: Observational analysis of a Mediterranean ‘hurricane’ over south-eastern Italy, *Weather*, 63, 306, 2008.
- Munsell, E. B., Zhang, F., and Stern, D. P.: Predictability and dynamics of a nonintensifying tropical storm: Erika (2009), *Journal of the atmospheric sciences*, 70, 2505–2524, 2013.
- 1285 Nastos, P., Papadimou, K. K., and Matsangouras, I.: Mediterranean tropical-like cyclones: Impacts and composite daily means and anomalies of synoptic patterns, *Atmospheric Research*, 208, 156–166, 2018.
- Noyelle, R., Ulbrich, U., Becker, N., and Meredith, E. P.: Assessing the impact of sea surface temperatures on a simulated medicane using ensemble simulations, *Natural Hazards and Earth System Sciences*, 19, 941–955, 2019.
- 1290 Ollinaho, P., Lock, S.-J., Leutbecher, M., Bechtold, P., Beljaars, A., Bozzo, A., Forbes, R. M., Haiden, T., Hogan, R. J., and Sandu, I.: Stochastically Perturbed Parametrizations (SPP)-representing model uncertainties on the process-level, in: *EGU General Assembly Conference Abstracts*, p. 17706, 2017a.
- Ollinaho, P., Lock, S.-J., Leutbecher, M., Bechtold, P., Beljaars, A., Bozzo, A., Forbes, R. M., Haiden, T., Hogan, R. J., and Sandu, I.: Towards process-level representation of model uncertainties: stochastically perturbed parametrizations in the ECMWF ensemble, *Quarterly Journal of the Royal Meteorological Society*, 143, 408–422, 2017b.
- 1295

- Palmen, E.: On the formation and structure of tropical hurricanes, *Geophysica*, 3, 26–38, 1948.
- Palmer, T. N., Buizza, R., Doblas-Reyes, F., Jung, T., Leutbecher, M., Shutts, G. J., Steinheimer, M., and Weisheimer, A.: Stochastic parametrization and model uncertainty, 2009.
- 1300 Panegrossi, G., D’Adderio, L. P., Dafis, S., Rysman, J.-F., Casella, D., Dietrich, S., and Sanò, P.: Warm Core and Deep Convection in Medicanes: A Passive Microwave-Based Investigation, *Remote Sensing*, 15, 2838, 2023.
- Pantillon, F., Chaboureaud, J.-P., Mascart, P., and Lac, C.: Predictability of a Mediterranean tropical-like storm downstream of the extratropical transition of Hurricane Helene (2006), *Monthly Weather Review*, 141, 1943–1962, 2013.
- Peinó, E., Bech, J., and Udina, M.: Performance Assessment of GPM IMERG Products at Different Time Resolutions, Climatic Areas and Topographic Conditions in Catalonia, *Remote Sensing*, 14, 5085, 2022.
- 1305 Picornell, M., Campins, J., and Jansà, A.: Detection and thermal description of medicanes from numerical simulation, *Natural Hazards and Earth System Sciences*, 14, 1059–1070, 2014.
- Portmann, R., González-Alemán, J. J., Sprenger, M., and Wernli, H.: How an uncertain short-wave perturbation on the North Atlantic wave guide affects the forecast of an intense Mediterranean cyclone (Medicane Zorbas), *Weather and Climate Dynamics*, 1, 597–615, 2020.
- Pytharoulis, I.: Analysis of a Mediterranean tropical-like cyclone and its sensitivity to the sea surface temperatures, *Atmospheric Research*, 1310 208, 167–179, 2018.
- Pytharoulis, I., Craig, G. C., and Ballard, S. P.: The hurricane-like Mediterranean cyclone of January 1995, *Meteorological Applications: A journal of forecasting, practical applications, training techniques and modelling*, 7, 261–279, 2000.
- Rabier, F., Järvinen, H., Klinker, E., Mahfouf, J.-F., and Simmons, A.: The ECMWF operational implementation of four-dimensional variational assimilation. I: Experimental results with simplified physics, *Quarterly Journal of the Royal Meteorological Society*, 126, 1143–1315 1170, 2000.
- Ragone, F., Mariotti, M., Parodi, A., Von Hardenberg, J., and Pasquero, C.: A climatological study of western mediterranean medicanes in numerical simulations with explicit and parameterized convection, *Atmosphere*, 9, 397, 2018.
- Rasmussen, E. and Zick, C.: A subsynoptic vortex over the Mediterranean with some resemblance to polar lows, *Tellus A*, 39, 408–425, 1987.
- 1320 Raveh-Rubin, S. and Flaounas, E.: A dynamical link between deep Atlantic extratropical cyclones and intense Mediterranean cyclones, *Atmospheric Science Letters*, 18, 215–221, 2017.
- Ricchi, A., Miglietta, M. M., Bonaldo, D., Cioni, G., Rizza, U., and Carniel, S.: Multi-physics ensemble versus atmosphere–ocean coupled model simulations for a tropical-like cyclone in the Mediterranean Sea, *Atmosphere*, 10, 202, 2019.
- Romero, R. and Emanuel, K.: Medicane risk in a changing climate, *Journal of Geophysical Research: Atmospheres*, 118, 5992–6001, 2013.
- 1325 Tiedtke, M.: A comprehensive mass flux scheme for cumulus parameterization in large-scale models, *Monthly weather review*, 117, 1779–1800, 1989.
- Tiedtke, M.: Representation of clouds in large-scale models, *Monthly Weather Review*, 121, 3040–3061, 1993.
- Torn, R. D. and Cook, D.: The role of vortex and environment errors in genesis forecasts of Hurricanes Danielle and Karl (2010), *Monthly weather review*, 141, 232–251, 2013.
- 1330 Vich, M., Romero, R., and Brooks, H.: Ensemble prediction of Mediterranean high-impact events using potential vorticity perturbations. Part I: Comparison against the multiphysics approach, *Atmospheric research*, 102, 227–241, 2011.

- Wimmer, M., Rivière, G., Arbogast, P., Piriou, J.-M., Delanoë, J., Labadie, C., Cazenave, Q., and Pelon, J.: Diabatic processes modulating the vertical structure of the jet stream above the cold front of an extratropical cyclone: sensitivity to deep convection schemes, *Weather and Climate Dynamics*, 3, 863–882, 2022.
- 1335 Yanai, M., Esbensen, S., and Chu, J.-H.: Determination of bulk properties of tropical cloud clusters from large-scale heat and moisture budgets, *Journal of Atmospheric Sciences*, 30, 611–627, 1973.
- Zhang, W., Villarini, G., Vecchi, G. A., and Murakami, H.: Rainfall from tropical cyclones: high-resolution simulations and seasonal forecasts, *Climate dynamics*, 52, 5269–5289, 2019.
- Zhang, W., Villarini, G., Scoccimarro, E., and Napolitano, F.: Examining the precipitation associated with medicanes in the high-resolution
1340 ERA-5 reanalysis data, *International Journal of Climatology*, 41, E126–E132, 2021.
- Zimbo, F., Ingemi, D., and Guidi, G.: The tropical-like cyclone “ianos” in September 2020, *Meteorology*, 1, 29–44, 2022.